Quaternary Science Reviews 340 (2024) 108867

Contents lists available at ScienceDirect

Quaternary Science Reviews

journal homepage: www.elsevier.com/locate/quascirev

Vegetation and fire history of the Lake Baikal Region since 32 ka BP reconstructed through microcharcoal and pollen analysis of lake sediment from Cis- and Trans-Baikal

Aleksandra I. Krikunova [a,**], Franziska Kobe [a], Tengwen Long [b,c], Christian Leipe [a,d,e], Jana Gliwa [a], Alexander A. Shchetnikov [f,g], Pascal Olschewski [a,h], Philipp Hoelzmann [i], Mayke Wagner [j], Elena V. Bezrukova [f], Pavel E. Tarasov [a,*]

[a] Institute of Geological Sciences, Palaeontology Section, Freie Universität Berlin, Malteserstraße 74–100, Building D, 12249, Berlin, Germany
[b] School of Geographical Sciences, University of Nottingham Ningbo China, 199 Taikang East Road, Yinzhou District, Ningbo, Zhejiang, 315100, China
[c] Key Laboratory of Carbonaceous Wastes Processing and Process Intensification Research of Zhejiang Province, University of Nottingham Ningbo China, 199 Taikang East Road, Yinzhou District, Ningbo, Zhejiang, 315100, China
[d] Domestication and Anthropogenic Evolution Research Group, Max Planck Institute of Geoanthropology, Kahlaische Str. 10, 07745, Jena, Germany
[e] Department of Archaeology, Max Planck Institute of Geoanthropology, Kahlaische Str. 10, 07745 Jena, Germany
[f] A.P. Vinogradov Institute of Geochemistry, Siberian Branch of the Russian Academy of Sciences, Favorskogo Str. 1a, Irkutsk, 664033, Russia
[g] Institute of the Earth's Crust, Siberian Branch of the Russian Academy of Sciences, Lermontova Str. 128, Irkutsk 664033, Russia
[h] Memorial University of Newfoundland, Department of Earth Sciences, 9 Arctic Avenue, A1B 3X5, St. John's, NL, Canada
[i] Institute of Geographical Sciences, Physical Geography, Freie Universität Berlin, Malteserstraße 74–100, Building B, 12249, Berlin, Germany
[j] Eurasia Department and Beijing Branch Office, German Archaeological Institute, Im Dol 2–6, 14195, Berlin, Germany

ARTICLE INFO

Handling editor: Yan Zhao

Keywords:
Vegetation cover
Wildfire
Last Glacial Maximum
Lateglacial-Holocene transition
Siberia
AMS dating

ABSTRACT

With the increase in global wildfire activity in response to global climate warming, the reconstruction of long-term fire histories and their links to environmental and anthropogenic factors has recently become an important focus of palaeoenvironmental research. Here we compare the precisely radiocarbon (^{14}C) dated long-term histories of vegetation change and fire activity from lakes Ochaul (Cis-Baikal) and Kotokel (Trans-Baikal) in the Lake Baikal Region (LBR) of Siberia, a known source region of wildfires whose past and future relationships with climate, vegetation structure and human economy are still poorly understood. Our results show that under cold and dry glacial climate conditions (32–18.2 ka BP) fire frequencies in both study regions were low. Deglaciation, which was characterised by the spread of woody plants, began around 18.2 ka BP, accompanied by a slight increase in fire activity. Differences in the fire records from both subregions are observed from the end of the Lateglacial (LG), with peak fire activity in Cis-Baikal during the Early Holocene (EH) and in Trans-Baikal during the Middle Holocene (MH). During the Late Holocene (LH) both regions are marked by generally low fire activity. We propose that the long-term spatiotemporal differences in fire activity during the EH–MH interval are primarily driven by vegetation composition and landscape openness and the resulting changes in fire regime. Interestingly, both peaks are also observed in a global-scale fire record, which suggests spatiotemporal complexity of the Holocene fire history. Low charcoal accumulation rates in both records during the Middle Neolithic (ca. 6660–6050 a BP) "cultural hiatus" archaeologically documented for Cis-Baikal suggest an LBR-wide population decline. On the other hand, the spread of Late Bronze and Iron Age cultures into the LBR from 3.5 ka BP may have at least partly driven the increase in fire frequency around Lake Kotokel.

1. Introduction

Located in the southern part of Siberia (Fig. 1a), Lake Baikal (Fig. 1b) is the oldest and deepest lake in the world. It contains about 20% of the global unfrozen fresh water reserves and hosts a rich freshwater fauna, including a large number of endemic species (Galaziy, 1993). This

* Corresponding author.
** Corresponding author.
E-mail addresses: aleksandra.krikunova@fu-berlin.de (A.I. Krikunova), ptarasov@zedat.fu-berlin.de (P.E. Tarasov).

https://doi.org/10.1016/j.quascirev.2024.108867
Received 10 May 2024; Received in revised form 22 July 2024; Accepted 29 July 2024
Available online 9 August 2024

underscores the exceptional value of the Lake Baikal Region (LBR) for evolutionary science (Simonov et al., 2022) and secures its place on the UNESCO World Heritage List (https://whc.unesco.org/en/list/754). However, global warming of recent decades and increasing anthropogenic impact have caused a multitude of problems that are causing growing concern about the protection and preservation of the LBR environment (Bilgaev et al., 2021; Simonov et al., 2022). Because the modern climate in the LBR, outside the mountain ranges, varies from semi-humid to semi-arid (Alpat'ev et al., 1976; Kobe et al., 2020), the regional environment is particularly sensitive to changes in temperature and moisture supply (Kostrova et al., 2020). One of the most serious problems in the region, which includes vast and topographically complex areas of the Irkutsk Oblast (Cis-Baikal) and the Republic of Buryatia (Trans-Baikal), are wildfires threatening nature and people and releasing huge amounts of carbon into the atmosphere (e.g. Dixon, 2021). The risk of wildfires is high across the LBR, covered with boreal (taiga) forests, where tree cover makes up more than 80% of the territory (Fig. 1c). However, the 2001–2007 fires were widely distributed across the relatively dry south (De Groot et al., 2013; Safronov, 2020), where boreal forests occupy a smaller area and forest-steppe and steppe landscapes are more common (Galaziy, 1993).

Devastating wildfires are not limited to the LBR, but are a common problem for the mid-latitudes of Eurasia (Goldammer and Furyaev, 1996) and North America (Barrett et al., 2013; Halofsky et al., 2020), which has become aggravated in the 21st century (Barhoumi et al., 2021). However, recent studies show that modern fire regimes differ between North American (predominantly 'crown') and Eurasian (predominantly 'surface') boreal forests (De Groot et al., 2013). Reconstruction of the Holocene fire history in Central Yakutia, north of the LBR, suggests that temporal shifts in the fire regime from the crown to the surface may occur in the same region (Katamura et al., 2009).

Better understanding of the long-term impacts of wildfires on the boreal landscape, along with a robust assessment of the relationships between fires, regional climate and human activities (Blarquez et al., 2015), requires high-resolution and well-dated records, including data-model comparisons to draw more accurate conclusions (Hély et al., 2010). Intensive efforts to generate and discuss Holocene fire records have been undertaken in the boreal forest zone of Fennoscandia (e.g. Clear et al., 2014; Lankia et al., 2012; Magne et al., 2019), Northern Urals (e.g. Barhoumi et al., 2019, 2020), Northeast China and Mongolia (e.g. Wang et al., 2022) and Canada (e.g. Carcaillet et al., 2001; Hély et al., 2010; MacDonald et al., 1991; Talon et al., 2005). Siberia is a known source region of wildfires, which impacts on climate and air quality and their effects on mortality and the economy under present and near-future warming remain poorly understood (Yasunari et al., 2024). While a few studies address the fire history of the last one to two millennia (e.g. Eichler et al., 2011; Glückler et al., 2021; Lamentowicz et al., 2015; Z. Wang et al., 2021), little is known about the fire history of the entire Holocene period (Barhoumi et al., 2021; Glückler et al., 2022) or other interglacials. Wildfire records from the Late Pleistocene period, including the Lateglacial (LG) and the Last Glacial Maximum (LGM), are particularly rare (Shichi et al., 2009, 2013). Unlike the vast boreal regions of Europe and North America, the LBR was not covered by extensive ice sheets during the LGM, as indicated by existing geomorphological (Osipov et al., 2003; Osipov and Khlystov, 2010), botanical (Bezrukova et al., 2009; Kobe et al., 2022b), zoological (Khenzykhenova et al., 2019; Markova et al., 2015; Puzachenko et al., 2017; Shchetnikov et al., 2015) and archaeological records (Dolukhanov et al., 2002; Fiedel and Kuzmin, 2007; Lbova, 2009; Vasil'ev et al., 2002). Major vegetation changes during the Late Pleistocene–Holocene interval and uninterrupted habitation by anatomically modern humans since the Upper Palaeolithic (Chlachula, 2017; Weber, 2020) make the area around Lake Baikal promising for the study of long-term changes in wildfire regimes and the complex interactions between fire, vegetation, climate and

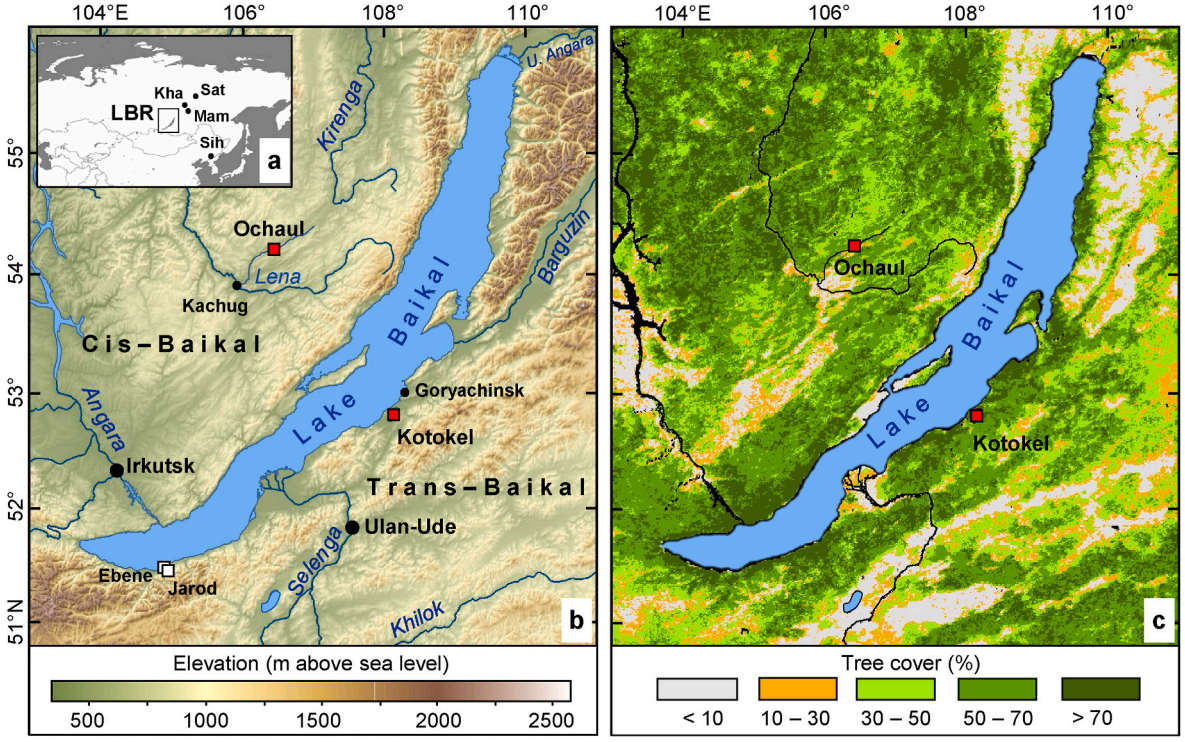

Fig. 1. (a) Map showing the location of the Lake Baikal Region (LBR: black rectangle), Lake Sihailongwan (Sih), Lake Satagay (Sat), Lake Khamra (Kha) and Mamakan Peat (Mam) in northern Asia; (b) Topographic map of the LBR with modern hydrology and location of the studied lakes Ochaul and Kotokel. White squares indicate the location of other key sites mentioned in the text and black dots represent modern cities. Topographic information is based on 90-m resolution Shuttle Radar Topography Mission (SRTM) v4.1 data (Jarvis et al., 2008); and (c) AVHRR-based modern tree cover (DeFries et al., 2000) in the LBR (maps in b and c after Kobe et al., 2020 with modifications).

human populations (Tarasov et al., 2021).

In this paper we present the results of microcharcoal and pollen analyses of two Accelerator Mass Spectrometry (AMS) radiocarbon-dated sediment cores from Lake Ochaul in Cis-Baikal and Lake Kotokel in Trans-Baikal. These results, which cover the past ca. 32 ka, are discussed with regard to the fire and environmental history of the two subregions. Furthermore, the reconstructed changes are compared with published archaeological records of human occupation.

2. Data and methods

2.1. Study sites and analysed cores

2.1.1. Lake Ochaul

Freshwater Lake Ochaul (Fig. 2a; 54.23°N, 106.47°E; 641 m a.s.l.) is located in the upper reaches of the Lena River, about 100 km northwest of Lake Baikal (Fig. 1b). It has a maximum length of ca. 2.7 km, a maximum width of ca. 1.2 km (Boyarkin, 2007) and a maximum water depth of about 2.5 m in its central part (Kobe et al., 2022a). The lake is

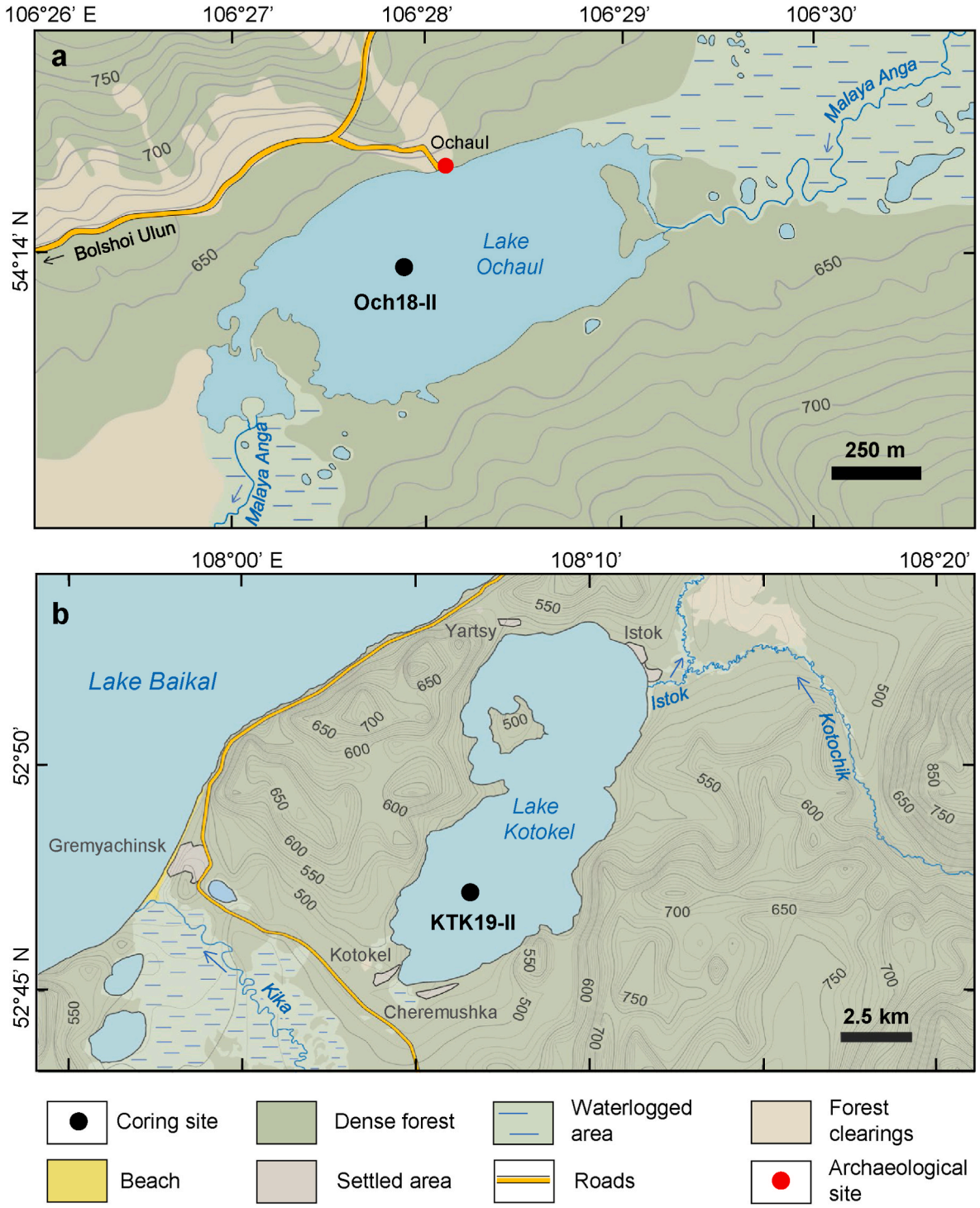

Fig. 2. Topographic maps of (a) Lake Ochaul and (b) Lake Kotokel indicating the location of the bottom sediment cores discussed in this study.

situated in a trough-shaped valley drained by the Malaya Anga River, which flows to the Bol'shaya Anga River – a right tributary of the Lena River (Fig. 1b). The valley floor is flat and swampy (Fig. 2a), and the slopes are covered with larch-dominated (*Larix*) boreal forest, which also consists of abundant birch (*Betula* sect. *Albae*) and Siberian pine (*Pinus sibirica*) trees, with admixture of spruce (*Picea obovata*) and fir (*Abies sibirica*) (Kobe et al., 2022a). The undergrowth is represented by shrubby birches (*Betula* sect. *Fruticosae* and *B.* sect. *Nanae*), shrubs of alder (*Alnus fruticosa*) and willow (*Salix*), diverse members of the heath family (Ericaceae), various herbaceous taxa, ferns and mosses (Belov et al., 2002). Meteorological data from Kachug (Fig. 1b) indicate a cold continental climate with high interannual variability in precipitation (212–480 mm; 318 mm on average) and mean January temperature (−36.3 to −24.1 °C; −28.4 °C on average) during the 1961–1990 interval, while the mean temperatures of July (+14.7 to +19.5 °C; +17.2 °C on average) and the year (from −5.2 to −2.4 °C; −4.0 °C on average) are less variable (http://www.pogodaiklimat.ru/history/30622.htm, accessed in April 2024).

The 7.24-m-long sediment core Och18-II (Fig. 3b) was recovered from the deepest part of the lake (Fig. 2a) in 2018 (see Kobe et al., 2022a, 2022b for details). The published age-depth model of the core based on extensive AMS ^{14}C dating (Fig. 3a) suggests lacustrine sediment accumulation during the past ca. 31.5 ka (Kobe et al., 2022b).

Earlier studies of the Och18-II core were focused on the past 13.5 ka (e.g. Kobe et al., 2022a) and the LGM interval from ca. 27.85 to 20.4 ka BP at centennial resolution (Kobe et al., 2022b) and reported results of sediment geochemistry, pollen and ostracod analyses and zooarchaeological data from a coastal archaeological site (Fig. 2a), which allowed to discuss changes in terrestrial vegetation, lacustrine environments and hunter-gatherer habitation history of the Upper Lena (Kobe et al., 2022a). In this paper, the published chronology and results of pollen analysis are combined with new results obtained for the remaining part of the Och18-II core.

2.1.2. Lake Kotokel

Lake Kotokel (Fig. 2b; 52.49°N, 108.09°E; 458 m a.s.l.) is located about 2 km from the eastern shore of Lake Baikal and connected to the latter via the Istok, Kotochik and Turka river system (Kostrova et al., 2013). Lake Kotokel is a 15-km-long and approximately 6-km-wide basin, with an average depth of 4–4.5 m and a maximum depth of 15 m (Shchetnikov et al., 2022). The shoreline reflects the complex topography of the surrounding area (Fig. 2b) with alternating hills, low mountain ranges and floodplains.

The natural vegetation around the lake has been affected by recent human activities. A detailed study of vegetation structure was carried out in a better-preserved wetland southwest of the lake, known as the Cheremushka Bog (Fig. 2b). Its marshy area is covered with reed and sedge communities, low-growing birch trees and shrubs of the heath family. The elevated rocky ledges and aeolian sands outside the bog are covered with Scots pine (*Pinus sylvestris*) forests with admixture of larch and birch trees and heath semi-shrubs (e.g. *Ledum palustre* and *Vaccinium uliginosum*) in the understory (Shichi et al., 2009). Boreal evergreen conifer forests with Siberian pine, fir and spruce grow on the mountain slopes of Ulan-Burgasy south of the lake. At altitudes above 1800 m, mountain taiga gives way to birch and larch forests and shrub communities with *Pinus pumila*, *Alnus fruticosa* and *Betula middendorfii* (Bezrukova et al., 2010), while in the semi-arid, lower parts of the region (Fig. 1b), steppe vegetation is widespread (Fig. 1c).

Meteorological observations from the Goryachinsk weather station (Fig. 1b), situated ca. 15 km northeast of Kotokel, reveal an annual precipitation of 396 mm, an average January temperature of −18.1 °C and an average July temperature of +14.3 °C for the period 1961–1990 (http://www.pogodaiklimat.ru/history/30731.htm, accessed in April 2024). These values indicate a less continental climate compared to Lake Ochaul and the Trans-Baikal area to the south and east, which can be explained by the strong influence of Lake Baikal on the local climate (Galaziy, 1993).

Over the past two decades, Lake Kotokel and the coastal Cheremushka Bog have been cored several times for the purpose of

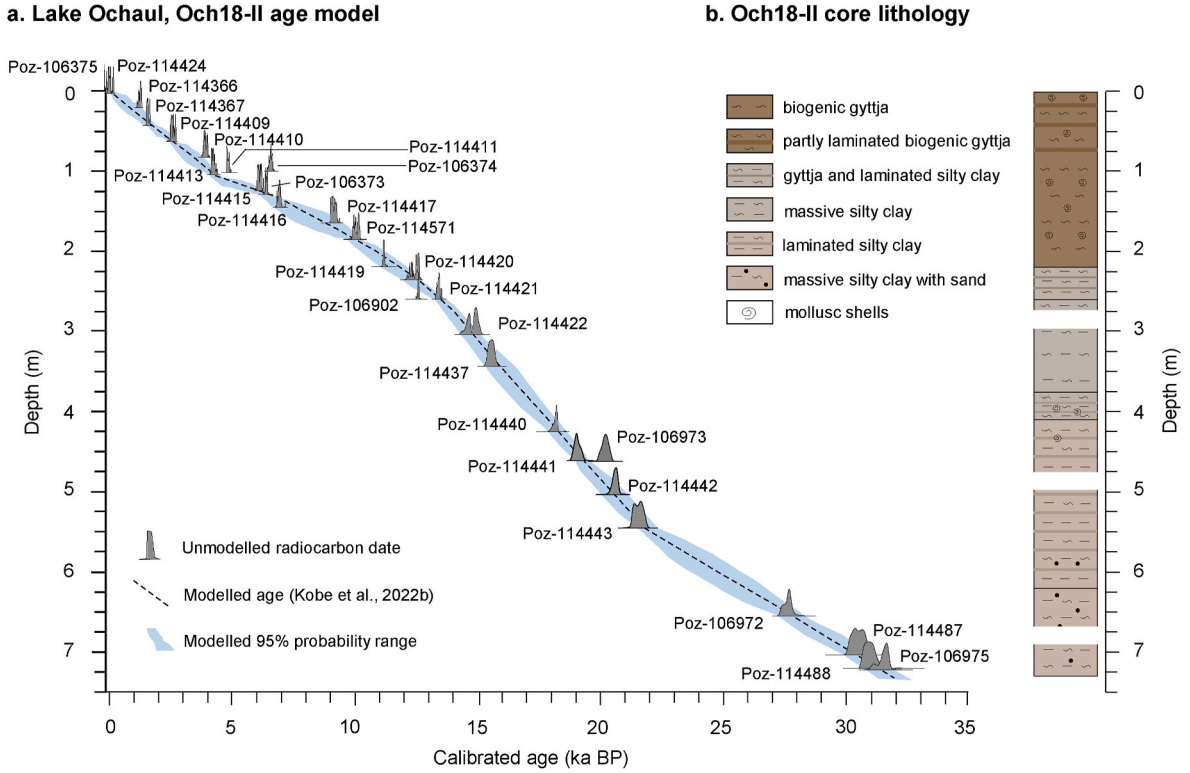

Fig. 3. (a) Age-depth model and (b) lithology of the Och18-II sediment core.

palaeoenvironmental reconstructions using a set of biological and geochemical proxies (Bezrukova et al., 2010; Fedotov et al., 2012; Kostrova et al., 2013; Müller et al., 2014; Shichi et al., 2009; Tarasov et al., 2019). Despite the progress in understanding the climate and vegetation history of the region made by previous studies, the age of published records based on a limited number of ^{14}C dates remains ambiguous.

In 2019, the so far longest available sediment core from Lake Kotokel (KTK19-II, Fig. 4b), measuring 14.5 m in length, was recovered from a depth of 3.6 m in the southern part of the lake (Fig. 2b) with an almost flat bottom and the thickest layer of undisturbed sediments (Zhang et al., 2013). The core was studied for palaeomagnetic properties, but not directly dated (Shchetnikov et al., 2022). The current paper presents a new chronology for the KTK19-II core based on a representative set of sediment samples dated in the Poznań Radiocarbon Laboratory and the results of pollen and microcharcoal analyses of the core.

2.2. ^{14}C dating and chronology of the KTK19-II core

A total of 26 bulk sediment samples from KTK19-II (Table 1) were submitted to the Poznań Radiocarbon Laboratory and ^{14}C-dated using the AMS technique. We calibrated all reported ^{14}C ages using the IntCal20 calibration curve (Reimer et al., 2020) in OxCal v4.4 (Bronk Ramsey, 1995). To model the age-depth relationship of the sequence (Fig. 4a), we employed the rbacon software package v3.2.0 (Blaauw and Christen, 2011) in the R v4.3.2 platform (R Core Team, 2016). The rbacon package uses Bayesian approaches for chronological modelling, allowing for inclusion of prior knowledge about the changes in stratigraphy or sedimentation rate (Wang et al., 2019). The top of the sequence (i.e. 0 cm depth) was constrained to −69 a BP, corresponding to the year 2019 CE when the core was recovered. Several dates from the lower part of the sequence exhibited obvious age-depth reversals and were excluded from the model. A more thorough examination in the Poznań Radiocarbon Laboratory revealed that these samples contain relatively large amounts of organic particles, likely reworked from older sediments. The most obvious reason for this was greatly increased soil erosion rates in the lake catchment, which coincided with decreasing temperatures at the end of Marine Isotope Stage (MIS) 3 (e.g. Marshall et al., 2017). To avoid inadequate age control and contamination by reworked older palynomorphs, we did not analyse the lower part of the KTK19-II core between 14.5 and 10.3 m and restricted the pollen and microcharcoal analyses to the upper 10.3 m.

2.3. Pollen and microcharcoal analyses

Extraction of pollen, cryptogam spores and microcharcoal particles was carried out following the protocol described in Leipe et al. (2019). It includes treatment of a given sediment sample with 10% HCl, 10% KOH, dense media separation using sodium polytungstate (SPT) at a density of 2.1 g/cm^3 and following acetolysis. In order to estimate palynomorph concentrations (Stockmarr, 1971) and accumulation rates (Knight et al., 2022), a known quantity of exotic *Lycopodium clavatum* marker spores was added to each sample prior to further chemical treatment. All palynomorphs were counted using a light microscope at 400× magnification. Taxonomic identification of pollen and cryptogam spores was carried out using available pollen atlases (Beug, 2004; Reille, 1992, 1995, 1998; Savelieva et al., 2013) and a reference collection. This protocol was already applied to 124 samples, which represent the LGM (Kobe et al., 2022a) and LG-Holocene (Kobe et al., 2022b) sections of the Och18-II core covering ca. 27.85 to 20.4 ka BP and the past 13.5 ka, respectively. In the current study we added another 47 samples, each representing a 1-cm-thick sediment layer, from not yet analysed parts of Och18-II for pollen analysis. Finally, microcharcoal particles, used as a fire proxy (Clark, 1988a; Tinner et al., 1998; Whitlock and Larsen, 2001), were counted in all 171 palynologically analysed samples, spanning the entire sediment sequence. For the purposes of this study, pollen, spores and charcoal particles were also counted in a total of 104 sediment samples from the upper 10.3 m of KTK19-II.

The charcoal particles were categorised into three size classes (10–50 μm, 50–100 μm and >100 μm) based on measurement of the longest axis of each particle. Larger charcoal particles (>100 μm) tend to be deposited close to their source, whereas smaller particles (<100 μm) can travel farther, generally reflecting regional fire sources (Clark, 1988b; Clark et al., 1998; Ohlson and Tryterud, 2000). Duffin et al.

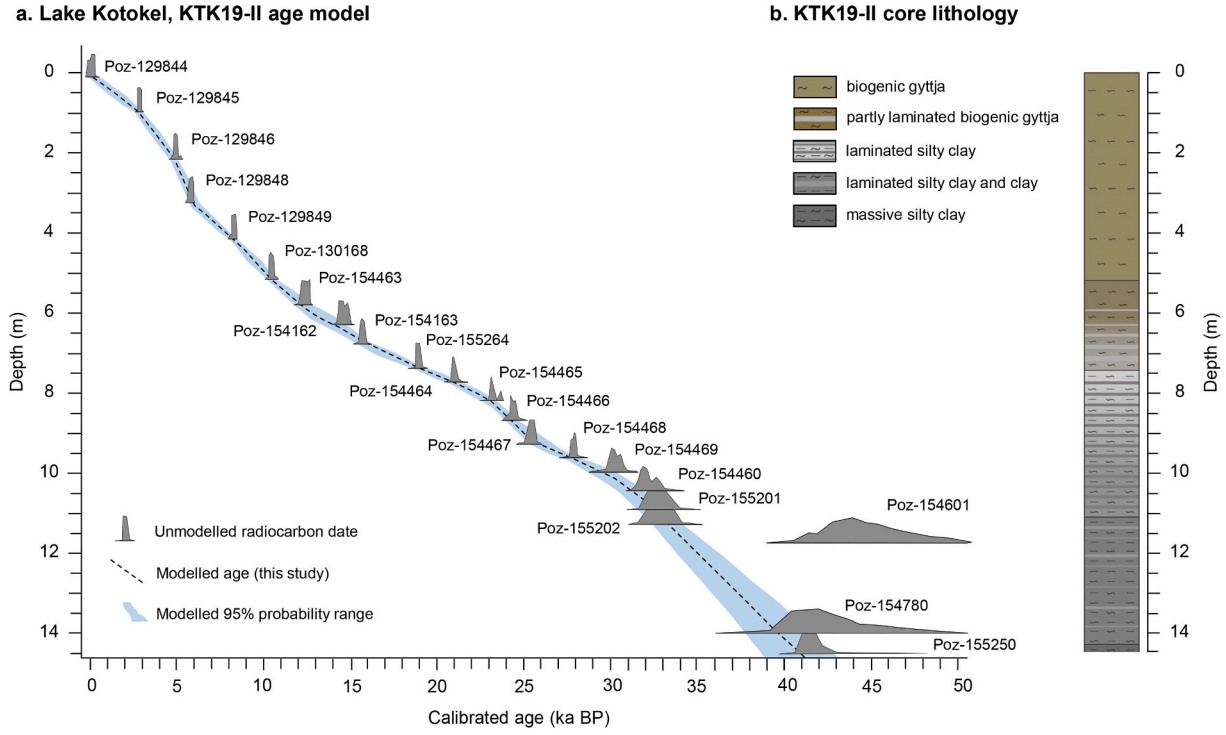

Fig. 4. (a) Age-depth model and (b) lithology of the KTK19-II sediment core.

Table 1
AMS ^{14}C dating results from the KTK19-II sediment sequence and their calibrated and modelled ages in 95% probabilistic range and median. The calibration is performed using OxCal v4.4 (Bronk Ramsey, 1995) and IntCal20 (Reimer et al., 2020).

Laboratory code	Depth (cm below core top)	^{14}C date (^{14}C a BP)	Calibrated age, 95% range (a BP)	Calibrated age, median (a BP)	Modelled age, 95% range (a BP)	Modelled age, median (a BP)
Poz-129844	8	195 ± 30	NA	184	300–−32	160
Poz-129845	96	2730 ± 30	2877–2759	2817	2920–2749	2811
Poz-129846	213	4350 ± 35	5035–4845	4918	4994–4556	4879
Poz-129848	321	5030 ± 35	5898–5660	5801	6428–5757	5883
Poz-129849	413	7430 ± 35	8343–8180	8263	8358–8058	8252
Poz-130168	513	9190 ± 50	10499–10240	10352	10629–10248	10396
Poz-154463	578	10440 ± 50	12615–12059	12337	12638–12085	12422
Poz-154162	629	12410 ± 60	14917–14210	14534	14779–14117	14385
Poz-154163	677	13090 ± 60	15911–15487	15693	16161–15527	15766
Poz-155264	737	15650 ± 80	19097–18795	18920	19223–18711	18924
Poz-154464	771	17370 ± 90	21341–20746	20957	21277–20567	20918
Poz-154465	819	19230 ± 110	23714–22940	23159	23315–22545	23043
Poz-154466	867	20260 ± 120	24697–23940	24346	24662–23941	24291
Poz-154467	927	21120 ± 140	25771–25158	25465	26656–25425	25759
Poz-154468	960	23450 ± 170	27856–27317	27615	28018–27257	27604
Poz-154469	996	26040 ± 310	31040–29852	30357	30262–28778	29497
Poz-154460	1044	28030 ± 300	33060–31336	32087	31899–30369	31330
Poz-155201	1092	28600 ± 420	34024–31777	32862	33210–31635	32474
Poz-155202	1126	28740 ± 420	34147–31905	33060	34064–32346	33276
Poz-154601	1174	43000 ± 2000	52322–42845	46363	35535–33317	34442
Poz-154782	1222	>44000	NA	NA	36840–34270	35539
Poz-154781	1258	>42000	NA	NA	37834–34988	36360
Poz-154778	1293	>43000	NA	NA	38796–35667	37169
Poz-155263	1341	>44000	NA	NA	40075–36652	38263
Poz-154780	1401	41000 ± 2000	50623–42016	44696	41634–37845	39655
Poz-155250	1449	40200 ± 1200	45586–42276	43664	42783–38746	40686

(2008) showed that particles larger than 50 μm are more strongly correlated with proximate fires, while smaller particles might signify fires on a regional scale or may not consistently indicate the occurrence of fire events. Charcoal particles smaller than 10 μm (i.e. <75 μm^2 in area) likely represent subcontinental or global sources (Clark, 1988b).

The macroscopic fraction of charcoal (>100 μm) was analysed using the stand-alone computer program CharAnalysis through MATLAB (Higuera et al., 2009), which divided the record into peaks representing fire (C_{peak}) and low charcoal frequency "non-fire" ($C_{background}$) episodes. Charcoal concentration was interpolated ($C_{interpolated}$) to produce equally spaced intervals (using the age-depth models shown in Figs. 3a and 4a), representing the median sample resolution of the records (i.e. 42 a/cm for Lake Ochaul and 28 a/cm for Lake Kotokel). This allowed the interpretation of the record in terms of charcoal accumulation rates (CHAR, particles/cm^2/a). $C_{background}$ was estimated using a locally weighted regression (lowess) with a 200-year window width for Lake Kotokel and a 250-year window width for Lake Ochaul, selected to maximise the signal-to-noise index (SNI) (Brossier et al., 2014). C_{peak} was calculated as the difference between $C_{interpolated}$ and $C_{background}$. The fire frequency and fire return interval (FRI, i.e. number of years between two fire events) were smoothed over a period of 1000 years.

Tilia v1.7.16 software (Grimm, 2011) was used for calculating terrestrial pollen and cryptogam taxa percentages and concentrations and drawing the diagrams for both Och18-II and KTK19-II records. For all analysed fossil samples calculated pollen taxa percentages refer to the sum of terrestrial pollen grains. When drawing the boundaries of bioclimatic zones, we followed internationally accepted age estimates (Cheng et al., 2020; Lisiecki and Raymo, 2005; Nakagawa et al., 2021; Walker et al., 2018).

2.4. Quantitative vegetation reconstruction

The quantitative pollen-based biome reconstruction approach (Prentice et al., 1996) allows objective interpretation of pollen data and facilitates comparisons between the individual records and the results of climate and vegetation modelling experiments (e.g. Kageyama et al., 2001; Prentice et al., 1992). Tests using representative modern reference pollen data from northern Eurasian have demonstrated the reliability of the method (e.g. Prentice and Webb III, 1998; Edwards et al., 2000; Mokhova et al., 2009; Tarasov et al., 1998) and justified its effectiveness for reconstructions of Late Pleistocene and Holocene vegetation of this large region (e.g. Binney et al., 2017). In the current study all terrestrial pollen taxa identified in the Och18-II and KTK19-II records were assigned to their corresponding plant functional types (PFTs) and biomes following the biome-taxon matrixes presented in recent publications reconstructing vegetation dynamics in Cis-Baikal (Kobe et al., 2022a, 2022b) and Trans-Baikal (Bezrukova et al., 2010; Kobe et al., 2020). The affinity scores for the natural potential biomes were calculated using an equation first published in Prentice et al. (1996).

Landscape openness was assessed by calculating the difference between the maximum forest biome score and the maximum open biome score calculated for each analysed spectrum (Tarasov et al., 2013). More recently, Abraham et al. (2021) used spatial patterns in recent total and arboreal pollen (AP) accumulation rates (PARs) across Europe as a tool for vegetation reconstruction. They showed that in a treeless landscape, at least 140 grains/cm^2/a can be found, and every 10% increase in forest cover leads to an increase in woody PAR by at least 400 grains/cm^2/a. Although a comparable study has not been conducted in the LBR, the published European dataset provides a qualitative tool to gain insights into forest dynamics and landscape openness around the studied lakes.

3. Results

3.1. Lake Ochaul

3.1.1. Chronology

The existing age-depth model for the Och18-II core (Fig. 3a; Kobe et al., 2022b) was used to date the not yet analysed sediment sections (Fig. 3b) at 724–700 cm (massive silty clay with sand) and 462–300 cm (massive, partly laminate silty clay). They represent the late MIS 3 and the early LG intervals and are dated to ca. 31.5–30 and 19.5–14.5 ka BP, respectively. According to the age model, each 1-cm-thick layer analysed represents an average interval of 45 years, and the interval between analysed samples varies from 45 to 180 years.

3.1.2. Fossil pollen assemblages and pollen-based biome reconstruction

The percentage diagram (Fig. 5) shows the detailed results of the pollen analysis, while the results of the pollen concentration/influx calculation and the biome/landscape openness reconstruction are presented in Fig. 6a and b, respectively. Based on the compositional changes in the Och18-II pollen assemblages, the record has been divided into seven zones, which correspond to the main bioclimatic phases of the last 31.5 ka. To facilitate further discussion the main characteristics of the selected zones shown in Figs. 5 and 6a and b are summarised in Table 2, starting with the MIS 3 (>29 ka BP) and continuing through the LGM (ca. 29–18.2 ka BP) interval, the LG climate amelioration phase, which ends with the Younger Dryas (YD) stadial (ca. 12.87 ka BP, Cheng et al., 2020), followed by the Early (EH: ca. 11.65–8.28 ka BP), Middle (MH: ca. 8.28–4.2 ka BP) and Late Holocene (LH: ca. 4.2 ka BP to present).

3.1.3. Microcharcoal analysis

The total concentration of microcharcoal particles in the analysed sediment samples and the charcoal accumulation rate (CHAR), calculated for various particle size categories, are presented in Fig. 6c. The total concentration is lowest during the MIS 3 and the LGM intervals, slightly higher during the LG and YD and shows a progressive increase to maximum values in the EH. The rest of the Holocene reveals moderately low concentrations comparable to that of the YD phase. The total CHAR shows similar trends, but there are some differences in absolute values and patterns of change between different charcoal fractions (Fig. 6c). The smallest size category accounts for the vast majority of charcoal particles counted (i.e. 90.3–97.4%). Medium and large-size particles account for up to 8.1% and 0–3.6%, respectively, with the most pronounced peaks between 13 and 8 ka BP.

3.2. Lake Kotokel

3.2.1. Chronology

The age-depth model for the analysed part of KTK19-II (Fig. 4) indicates that the upper 10.3 m of the studied core covers the last ca. 30.7 ka. According to the age model, the 1-cm-thick sediment layer represents an average time interval of 30 years, while the interval between analysed samples varies from 150 to 300 years.

3.2.2. Fossil pollen assemblages and pollen-based biome reconstruction

The detailed results of the pollen analysis of the KTK19-II core are shown in the pollen percentage diagram (Fig. 7). The pollen concentration/influx values and the biome/landscape openness reconstruction results are presented in Fig. 8a and b, respectively. Based on changes in the composition of pollen assemblages, the KTK19-II record is divided into seven bioclimatic zones for comparison with the Och18-II record. The main characteristics of the selected zones are summarised in Table 3.

One notable feature of the KTK19-II core is that the median age for the palynological layer indicating the start of the YD stadial, modelled at approximately 13.42 ka BP (Fig. 4a), appears slightly older than the commonly accepted age for the YD onset, which is around 12.87 ka BP (Cheng et al., 2020). However, the lower limit of the 95% confidence interval for the modelled age (Table 3) is close to the recognised start of the YD, suggesting that the observed discrepancy falls within the range of uncertainty. This deviation can be explained by a minor contribution of older carbon material to the dated sediment during the interstadial to stadial transition.

3.2.3. Microcharcoal analysis

The total concentration of microcharcoal particles and the charcoal accumulation rate in the sediment samples of the KTK19-II are shown in Fig. 8c. The total concentration shows the lowest values during the MIS 3 and the LGM intervals and an increasing trend towards the maximum

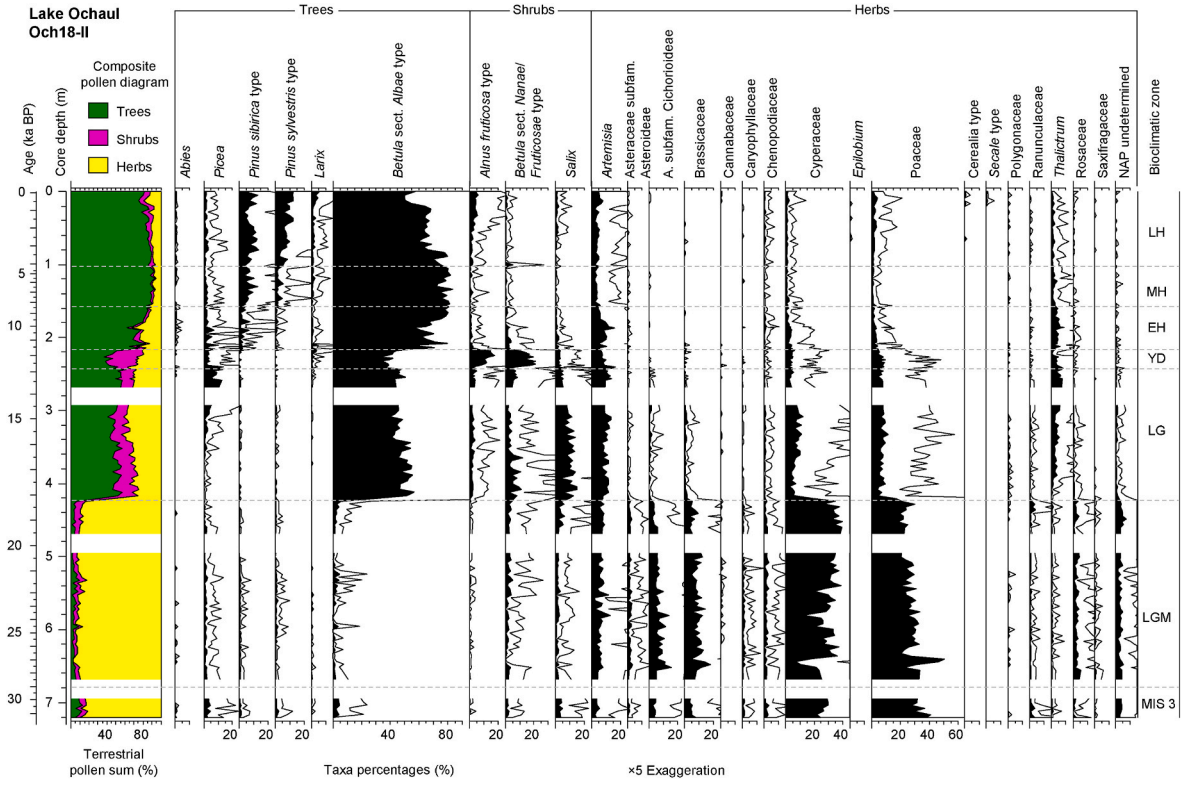

Fig. 5. Percentage diagram of the Och18-II pollen record plotted against the core depth and age axes. Dashed horizontal lines indicate the boundaries of the bioclimatic zones discussed in the text. White stripes indicate gaps in the recovered sediment core, resulting in a discontinuity in the analytical records.

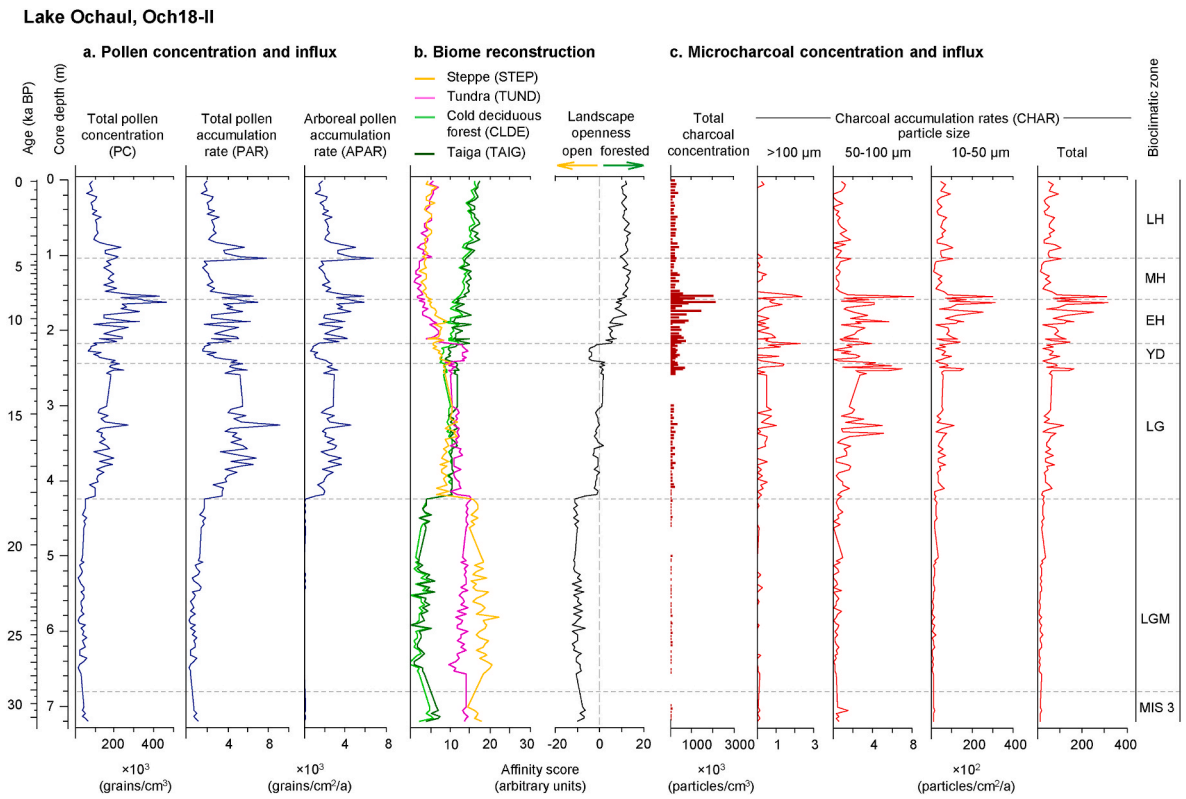

Fig. 6. Pollen and microcharcoal concentrations and accumulation rates, results of biome score calculation and landscape openness derived from the Och18-II core sediment.

values during the early MH ca. 8–7 ka BP. The charcoal concentration values then fall again and remain at a medium level until the present. The total CHAR curve shows similar trends between 30.7 and 8 ka BP, however, maximum values occur between 5.8 and 4.9 ka BP (Fig. 8c). The smallest size category accounts for the vast majority of charcoal particles counted (i.e. 85.1–100%). Medium and large-size particles account for up to 13.4% and 0–5.9%, respectively.

4. Discussion

4.1. Vegetation history of the LBR: general trends and new insights

The robustly dated and consistently analysed Och18-II and KTK19-II pollen records presented here provide an excellent opportunity to reconstruct and compare the vegetation history of Cis- and Trans-Baikal over the last 32 ka. Temporal changes in the composite pollen diagrams (Figs. 5 and 7) demonstrate a number of similarities between the two records, including (i) very low percentages of tree and shrub taxa during the LGM interval; (ii) gradual expansion of woody plants (mainly birches) in both subregions after ca. 18.2 ka BP; (iii) a noticeable peak in shrub pollen (mainly alder) during the YD; (iv) maximum percentages of tree pollen during the MH; and (v) increased contribution of shrub and herbaceous pollen in the LH. These changes in pollen composition are well reflected in affinity scores of regional biomes and landscape openness. The current results provide new insights into the Late Quaternary vegetation history of the LBR, presented in earlier studies of the two lakes (e.g. Bezrukova et al., 2010; Kobe et al., 2022a, 2022b; Müller et al., 2014), and offer a robust stratigraphic framework for other poorly dated palynological records from the region (e.g. Bezrukova et al., 2005, 2013, 2022; Fedotov et al., 2012; Mackay et al., 2013; Shichi et al., 2009). The latter records are particularly useful for continental and global scale reanalysis projects focusing on vegetation cover (e.g. Binney et al., 2017) and climate (e.g. Herzschuh et al., 2023) reconstructions, as well as for refining data-data and data-model vegetation comparisons (e.g. Chevalier et al., 2023).

The transition from MIS 3 to MIS 2 in the Ochaul and Kotokel records is clearly discernible by the change in the pollen composition and concentration values, as well as in the reconstructed biome scores (Figs. 5–8) and landscape openness (Fig. 9a). This transition corresponds to the internationally accepted date of ca. 29 ka BP estimated using a stack of 57 globally distributed benthic $\delta^{18}O$ records (Lisiecki and Raymo, 2005) and allows to adjust the earlier estimate of the MIS 3/2 boundary in the KTK2 record (Bezrukova et al., 2010).

The lowest AP percentage values and the highest scores of the steppe and tundra biomes in our LGM pollen records agree well with pollen and plant macrofossil data from different parts of Siberia, indicating the widespread dominance of herbaceous vegetation in the Asian high latitudes (e.g. Tarasov et al., 2021). This conclusion is supported by the studies of ancient environmental genomics (e.g. Y. Wang et al., 2021), which find a dominance of relatively homogeneous steppe–tundra vegetation in the Arctic during the LGM. However, the possible survival of cold-tolerant boreal trees and shrubs in isolated refugia during the LGM remains a discussion topic (e.g. Herzschuh, 2020; Müller et al., 2010), although there is various evidence for the existence of such refugia (e.g. Schulte et al., 2022; Tarasov et al., 2021). Recently, Kobe et al. (2022b) ruled out long-distance pollen transport as a main source of the AP found in the LGM sediment from Lake Ochaul and argued that the Upper Lena with the Cis-Baikal Depression, including the vicinity of Lake Ochaul, was a region in which scattered woods could survive the harsh glacial climate. The Tunka Valley southwest of Lake Baikal may be another place where isolated trees/shrubs could survive the LGM in favourable microhabitats. However, the exact location of these refugia cannot be determined without directly dated plant macrofossils.

The arboreal pollen accumulation rates (APAR) from the Och18-II (Fig. 6a) and KTK19-II (Fig. 8a) records are below 140 grains/cm^2/a during the LGM interval, which support a predominantly treeless LBR

Table 2
Characteristics of pollen assemblages and pollen-derived biomes in the Och18-II sediment core from Lake Ochaul.

Bioclimatic zone: core depth (cm); *modelled age* (95% range, a BP)	Assigned age (a BP)	Dominant taxa and characteristic features, including pollen concentrations (PC, grains/g and grains/cm^3), pollen accumulation rates (PAR, grains/cm^2/a), dominant biomes and landscape openness
MIS 3: 724–680; *32,105/31,150–29,910/28,415*	ca. 31,500–29,000	**Poaceae–Cyperaceae–Brassicaceae-Asteraceae** – Herbs are predominant (82–90%): Poaceae (27–41%), Cyperaceae (22–30%), Brassicaceae (3–8%), Asteraceae (4–6%), and *Artemisia* (2–5%). Woody taxa (e.g. *Picea*, *Pinus*, *Betula* and *Salix)* are scarce. PC (24,600 grains/g; 47,730 grains/cm^3) and PAR (870 grains/cm^2/a) averages are relatively low. The STEP and TUND biomes predominate in the landscape.
Last Glacial Maximum: 680–422; *29,910/28,415–18,491/17,829*	ca. 29,000–18,200	**Poaceae–Cyperaceae–Asteraceae–Brassicaceae** – Prevalence of herbaceous taxa increases (82–97%), including Poaceae (19–51%), Cyperaceae (7–40%), Asteraceae (5–18%), Brassicaceae (3–18%), and *Artemisia* (2–13%). The presence of boreal shrubs (*Salix* and *B.* sect. *Nanae/Fruticosae*) slightly elevates towards the upper part of the zone (up to 7% and 5%, respectively). Trees remain at minimum levels (1–10%). PC averages decline to 19,100 grains/g and 35,850 grains/cm^3, while PAR increases slightly to 920 grains/cm^2/a. The STEP biome shows highest affinity scores and the landscape openness slightly increases.
Lateglacial: 422–244; *18,491/17,829–13,092/12,367*	ca. 18,200–12,870	***B.* sect. *Albae*–Cyperaceae–*Artemisia*–Poaceae –** Proportion of arboreal pollen (30–61%) increases rapidly, primarily due to a significant rise in *B.* sect. *Albae* (29–57%). *Picea* advances in the upper part of the zone, with two peaks up to 14%. Boreal shrubs witness an increase (10–29%), comprising *Salix* (up to 15%), *B.* sect. *Nanae/Fruticosae* (up to 12%), and *Alnus fruticosa* (up to 5%). Herbaceous taxa decline from 55% to 37%, with Cyperaceae (2–19%), *Artemisia* (7–17%), and Poaceae (4–17%) experiencing slight rises in the midsection of the zone. *Thalictrum* rises in the upper part of the zone, reaching up to 8%. PC (94,000 grains/g; 146,650 grains/cm^3) and PAR (4660 grains/cm^2/a) averages increase rapidly as well. Several biomes reveal similar scores, indicating mosaic vegetation and an increased role of tree/shrub associations.
Younger Dryas: 244–217; *13,092/12,367–12,076/10,963*	ca. 12,870–11,650	***B.* sect. *Albae*–*B.* sect. *Nanae/Fruticosae*–*Alnus fruticosa*–*Artemisia* –** Pollen contribution from trees (37–51%), predominantly represented by *B.* sect. *Albae* (32–44%), decreases. *Picea* declines to 4%, while *Larix* appears in small quantities. The percentage of boreal shrubs increases (28–37%), with *B.* sect. *Nanae/Fruticosae* (10–21%) and *Alnus fruticosa* (8–18%) having the highest percentages in this zone. Contributions from herbaceous species continue to decrease (19–28%), including *Artemisia* (6–10%), Poaceae (5–10%), Cyperaceae (2–6%), and *Thalictrum* (up to 5%). PC (89,870 grains/g; 119,320 grains/cm^3) and PAR (2730 grains/cm^2/a) averages decreases. Return to TUND dominance and a more open landscape.
Early Holocene: 217–156; *12,076/10,963–9071/7290*	ca. 11,650–8280	***B.* sect. *Albae*–*Artemisia*–*Picea*–*Thalictrum* –** Amount of arboreal pollen (63–88%) increases, mainly attributed to *B.* sect. *Albae* (54–81%), *Picea* (up to 10%), and *Pinus sibirica* type (up to 7%). A few pollen grains of *Abies* appear discontinuously. The contribution of boreal shrubs (1–12%) declines rapidly, represented by *Alnus fruticosa* (up to 6%) and *B.* sect. *Nanae/Fruticosae* (up to 4%). Herbs slightly increase (11–32%), with peaks of *Artemisia* (5–16%) and *Thalictrum* (2–9%) in the middle part of the zone. Poaceae and Cyperaceae decrease to 2% towards the upper part. PC (173,900 grains/g; 222,400 grains/cm^3) averages are highest in this zone, while PAR averages (4030 grains/cm^2/a) increase. An increase in the TAIG and CLDE biome scores and a parallel decrease in the scores of TUND and STEP. Progressive afforestation of the landscape.
Middle Holocene: 156–103; *9071/7290–4380/4012*	ca. 8280–4200	***B.* sect. *Albae*–*Pinus*–*Artemisia*–*Thalictrum* –** Trees dominate the zone (88–93%), with *B.* sect. *Albae* (72–83%), *Pinus sibirica* type (3–13%), *Pinus sylvestris* type (1–5%), and *Larix* (up to 3%) being prominent, while *Picea* declines to 3%. Boreal shrubs have minimal influence (up to 5%). Herbaceous species decrease to 10%, including *Artemisia* (2–5%) and *Thalictrum* (1–4%). PC (157,300 grains/g; 216,420 grains/cm^3) averages decline, while PAR averages (4945 grains/cm^2/a) rich their highest in this zone. The TAIG and CLDE biomes predominate in the densely forested landscape.
Late Holocene: 103–0; *4380/4012–present*	ca. 4200– present	***B.* sect. *Albae*–*Pinus*–*Artemisia*–*Alnus fruticosa* –** Contribution from trees (75–90%) decreases towards the upper part of the zone, mainly due to the decline of *B.* sect. *Albae* from 80% to 57%. *Pinus sibirica* type (3–13%), *Pinus sylvestris* type (3–13%), *Larix* (up to 6%), and Picea (up to 3%) increase. The impact of boreal shrubs is low (1–8%), with *Alnus fruticosa* increasing in the upper part up to 6%. Herbaceous taxa slightly increase (up to 6–19%), with *Artemisia* (2–8%) and Poaceae (up to 4%) being notable. PC (86,000 grains/g; 116,000 grains/cm^3) and PAR (2930 grains/cm^2/a) averages decrease. The TAIG and CLDE biomes remain dominant, but the TUND and STEP biome scores show moderate increase accompanied by a slight increase in landscape openness.

landscape, based on the reference APAR data from Europe (Abraham et al., 2021). Although these results are consistent with the generally accepted interpretation, the European dataset may not be fully representative of Siberia and the LBR, where boreal forests contain large quantities of larch, whose pollen is known to be poorly represented, especially in lacustrine sediments (e.g. Müller et al., 2010). Sedimentary ancient DNA (sedaDNA) records from eight lakes located north of the LBR indicate that *Larix sibirica* had a wider eastern distribution around 33 ka BP and LGM samples consistently show *L. gmelinii* genotypes (Schulte et al., 2022). These independent records support the pollen- and plant macrofossil-based hypothesis (Kobe et al., 2022b; Müller et al., 2010; Tarasov et al., 2007) suggesting that Holocene boreal forests in Siberia are the result of "local expansion of small tree populations that survived the LGM in cryptic refugia" (Petit et al., 2008).

The majority of palynological and palaeoecological studies in the LBR focused primarily on the LG-Holocene transition and the Holocene, covering the past ca. 14.5 ka (e.g. Andreev and Tarasov, 2013; Barhoumi et al., 2021; Bezrukova et al., 2013; Demske et al., 2005; Kobe et al., 2022a). Our study shifts the focus to earlier periods, examining the response of regional vegetation to the onset of deglaciation as shown in global records (e.g. Jackson et al., 2019). The pollen records from Lake Ochaul and Lake Kotokel demonstrate a synchronous increase in pollen concentrations and PARs, along with an increase in AP after 18.2 ka BP. This suggests an improvement in the regional climate towards a warmer, wetter environment and spread of boreal trees and shrubs in the study areas (Fig. 9a). These changes towards less continental regional climate precede by more than three millennia the major shift in the NGRIP $\delta^{18}O$ record (Fig. 9d), known as the Bølling-Allerød (B-A) interstadial, which is particularly well-expressed in robustly dated pollen diagrams from Central Europe (e.g. Litt and Stebich, 1999; Litt et al., 2001) and Arctic Siberia (e.g. Andreev et al., 2004; Müller et al., 2010). The initial increase in the abundance of tree and shrub pollen in published records from the LBR is conventionally associated with the B-A interval between ca. 15 and 13 ka BP (Bezrukova et al., 2010; Demske et al., 2005; Shichi et al., 2009, 2013, 2023), but the LG chronologies of these records remain ambiguous.

A study of annually laminated sediments from Lake Sihailongwan in eastern Eurasia provides a high-resolution and accurately dated pollen and climate record of the last 65 ka (Mingram et al., 2018). This record shows a gradual increase in AP after 20 ka BP, with a maximum around 6 ka BP (Fig. 9b). This trend is reminiscent of the expansion of woody vegetation reflected in the Ochaul and Kotokel records of landscape openness (Fig. 9a) and coincides with increases in Northern Hemisphere summer insolation (Fig. 9f), global CO_2 concentrations (Fig. 9c) and sea

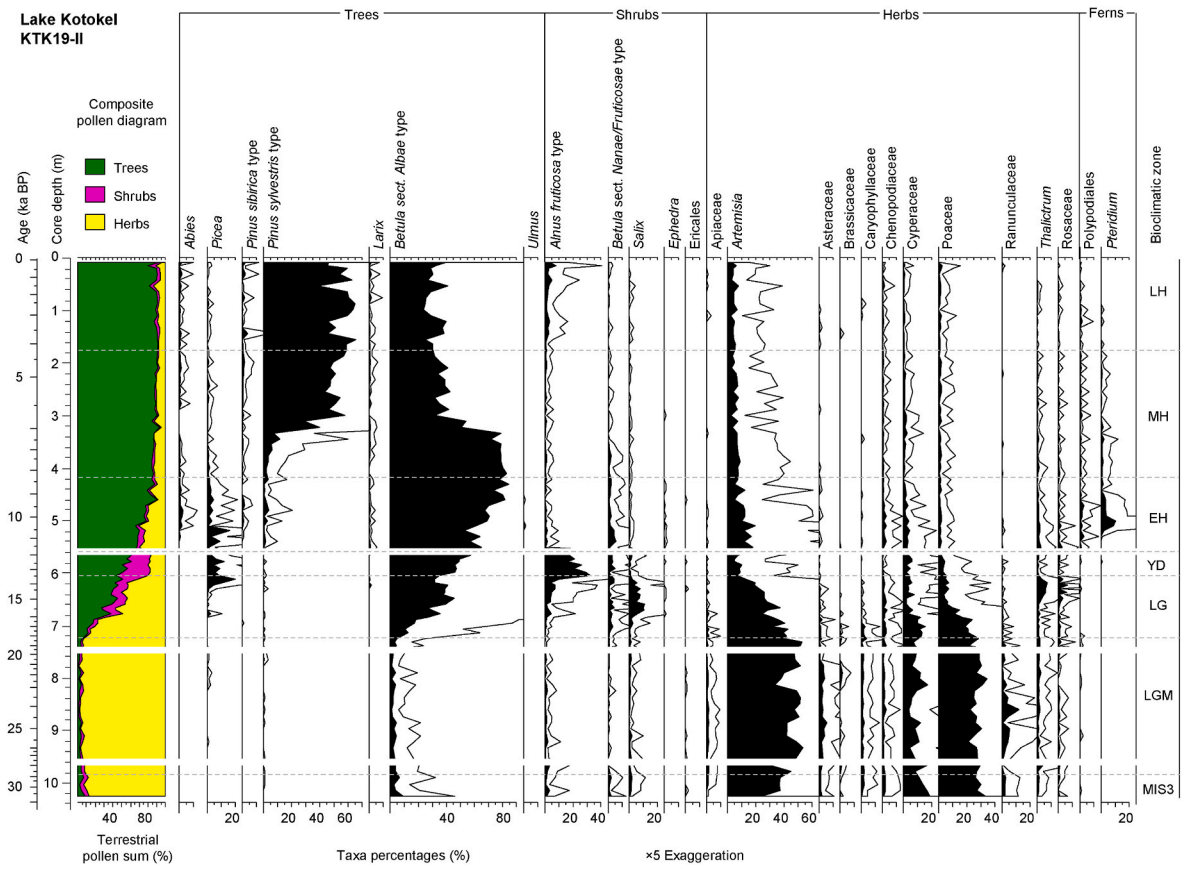

Fig. 7. Percentage diagram of the KTK19-II pollen record plotted against the core depth and age axes. Dashed horizontal lines indicate the boundaries of the bioclimatic zones discussed in the text. White stripes indicate gaps in the recovered sediment core, resulting in a discontinuity in the analytical records.

level (Fig. 9e), which precede the beginning of deglaciation in the European Alps (Ivy-Ochs et al., 2023) and easternmost Europe (Korsakova et al., 2023). Jackson et al. (2019) used tropical glacier fluctuations to estimate the timing of low-latitude temperature changes relative to global climate forcing and demonstrated that glacial retreat in the tropics had already begun by 20 ka BP before a rapid rise in CO_2 levels occurred ca. 18.2 ka BP. For the first time, the environmental impacts of "early warming" registered in the tropics and Northeast China can be reliably traced in the LBR, suggesting that mid-latitude East Asia was sensitive to rising summer insolation and decreasing global ice volume. The more rapid increase in the percentages of tree and shrub pollen in the Och18-II record compared to KTK19-II supports the idea of a glacial tree/shrub refugium around Lake Ochaul proposed by Kobe et al. (2022b) and can be adequately explained by the locally wetter environments, as evidenced by the lower proportion of *Artemisia* in comparison to Cyperaceae and Poaceae pollen (Kobe et al., 2022b).

4.2. Wildfire history

4.2.1. General trends

Charcoal analysis, which involves counting charcoal fragments in tandem with routine pollen analysis of lacustrine sediments, is used by palaeoecologists to evaluate past fire regimes (e.g. frequency and intensity of fires) or, more conservatively, the role of fire in shaping terrestrial ecosystems at different times and places (Clark, 1988b). The charcoal records from Lake Ochaul (Fig. 6c) and Lake Kotokel (Fig. 8c) allow comparison of the wildfire trends in Cis- and Trans-Baikal since the end of MIS 3. Both records demonstrate very low charcoal influx and concentration before ca. 18.2 ka BP and a moderate increase during the LG. The highest values are observed during the Early (ca. 9.5–8 ka BP; Lake Ochaul) and Middle (ca. 6–5 ka BP; Lake Kotokel) Holocene, followed by a decrease after 4.2 ka BP.

Following Tinner et al. (2005), who reconstructed fire ecology in the European Alps since the last ice age, we interpret low charcoal influx as indication of subdued fire activity in the LBR before 18.2 ka BP. However, low charcoal abundance in lacustrine sediments may also reflect particularities of the fire regime in a treeless ice age landscape, which remain understudied. For example, fire size and intensity play a decisive role in influencing the degree of combustion of herbaceous plant material (Whitlock and Larsen, 2001). On the one hand, it is likely that in steppe or tundra-steppe environments, where fuel supply is low and fires burn very efficiently, little charcoal is produced (e.g. Chipman et al., 2015; Higuera et al., 2011). On the other hand, records of historical fires from four lakes across the North American Great Plains indicate that prairie fires can produce significant amounts of charred herbaceous material (Umbanhowar, 1996). However, reduced productivity during drier periods (i.e. positive correlation between charcoal abundance and atmospheric precipitation) results in more patchy fuel distribution and fewer and/or smaller fires (Umbanhowar, 1996). More recent studies support this interpretation and suggest that grazing and trampling by large ungulates such as bison may alter fuel continuity and result in patchier burns (e.g. Zouhar, 2021). One can speculate that an open landscape with a relatively dry and cold climate (e.g., Bezrukova et al., 2010; Kobe et al., 2022b) and large herds of herbivorous animals (e.g., Markova et al., 2015; Puzachenko et al., 2017) that fed on and trampled aboveground biomass could be responsible for the low charcoal concentrations found in the lake sediment from the LBR during the last ice age. However, the lack of reliable information on the number of animals and their migration patterns, as well as the lack of palaeocharcoal records from the wider region, make it difficult to verify this hypothesis.

The improving LG climate and associated spread of woody vegetation across the LBR coincide with increasing charcoal influx in Och18-II

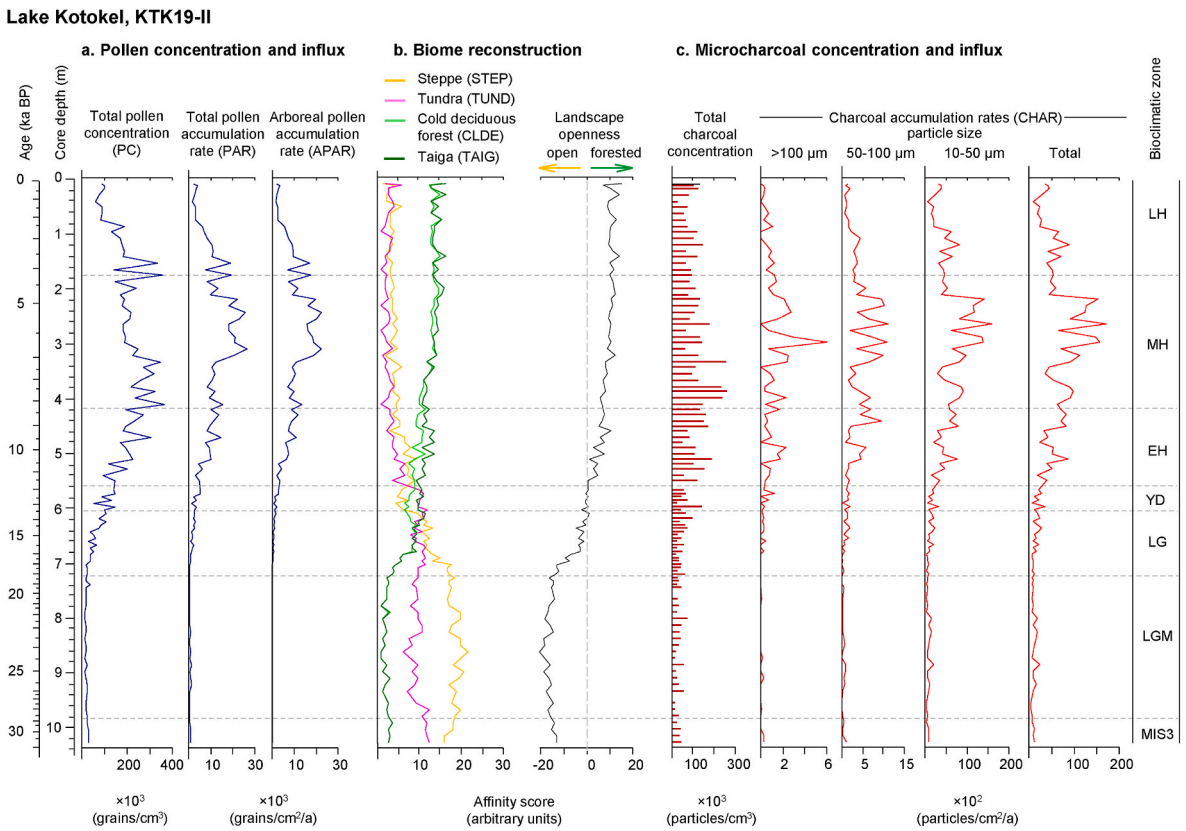

Fig. 8. Pollen and microcharcoal concentrations and accumulation rates, results of biome score calculation and landscape openness derived from the KTK19-II core sediment.

(Fig. 6c) and KTK19-II (Fig. 8c). These trends in the LBR records match well with the data from the lake region between the Jura Mountains and the Swiss Alps, where rapid increase in *Juniperus* at ca. 15.5 ka BP marked the beginning of afforestation (Tinner et al., 2005). Detailed quantitative analysis of the microcharcoal data shows peaks in fire frequency ca. 13.0 ka BP at Lake Ochaul (Fig. 9j) and ca. 13.5 ka BP at Lake Kotokel (Fig. 9k), which coincide with the B-A interstadial and spread of spruce in the region.

CHAR levels of the >100 µm fraction (Fig. 9h) remain relatively high during the Early Holocene in both the Ochaul and Kotokel records, suggesting high fire activity, although modelled fire frequency (Fig. 9j and k) decreases in both areas. Comparison with the published Holocene records from two small lakes (Ebene and Jarod, Fig. 1b) situated on the south-western shore of Baikal (Barhoumi et al., 2021) shows that peaks in fire frequency and magnitude between 10.5 and 10 ka BP and around 8 ka BP (Fig. 9l) are also reflected in the records obtained in our study (Fig. 9h). Intriguingly, the highest peak in the fire frequency reconstructed in Lake Ebene around 8 ka BP corroborates the high CHAR values in the Kotokel and Ochaul records. The latter could indicate the possible impact of the 8.2 ka BP event on the regional environments and fire ecology, although more data are needed to prove this hypothesis. Until now, the sensitivity of regional vegetation to the 8.2 ka climatic event has rarely been the focus of environmental studies in the LBR. Shichi et al. (2013) reported an increase in birch pollen and charcoal fragments in the VER99G12 core from Lake Baikal, which they linked to the 8.2 ka BP cooling. The remarkable increase in charcoal accumulation rate and the very rapid spread of pioneer vegetation, including birch and various herbs, were attributed to the influence of fire (Shichi et al., 2013). The terrestrial pollen records and pollen-based reconstructions presented here indicate that the 8.2 ka event is poorly represented by small peaks in the herbaceous pollen sum and a drop in total pollen concentrations (Fig. 5), indicating limited impact of the cooling event on the vegetation around lakes Ochaul and Kotokel. The stronger vegetation response observed in the VER99G12 dataset can be explained by the proximity of the core site to an area with drier climate and more sensitive environments (Galaziy, 1993).

The MH interval reveals maximum CHAR values from Lake Kotokel (Fig. 9g and h) between ca. 6 and 5 ka BP, synchronous with the increased fire frequency in the two other records from Trans-Baikal (Fig. 9l) and with a second Holocene peak in global charcoal abundance (Fig. 9m). However, the available records from lakes Ochaul (Fig. 9j) in Cis-Baikal and Satagay (Fig. 9i) in Central Yakutia (Glückler et al., 2022) show much lower values compared to the EH. The observed differences in the records north and south of Lake Baikal likely indicate regional differences in the fire regimes of the two regions during the Holocene, complicated by local fire variability. Intriguingly, the two observed regional peaks in the CHAR data from Cis- and Trans-Baikal have their respective counterparts in Early and Middle Holocene changes in the global fire and charcoal dataset (Fig. 9m), which unfortunately includes very few records from Northern Asia (Power et al., 2008, 2010).

The Ochaul and Kotokel records demonstrate relatively low CHAR levels in the Late Holocene, with a small increase over the last millennium. The CHAR record from Central Yakutia (Glückler et al., 2022) shows a similar picture (Fig. 9i), consistent with the decreasing trend in the global dataset (Fig. 9m). In contrast to the decreasing CHAR and fire magnitude, fire frequency increases from a minimum around 4 ka BP to peak values ca. 1–0.5 ka BP. This trend is most pronounced in the records from lakes Kotokel (Fig. 9k) and Jarod (Fig. 9l) in Trans-Baikal, but does not appear in the Ochaul record (Fig. 9j). Several short-term oscillations (including one at 1 ka BP) appear in the global fire dataset (Fig. 9m). Another Middle to Late Holocene palynological record from a peat section in the Mamakan River valley (Fig. 1a) shows landscape opening after a relative increase in fire activity between 3870 and 3820

Table 3
Characteristics of pollen assemblages and pollen-derived biomes in the KTK19-II sediment core from Lake Kotokel.

Bioclimatic zone: core depth (cm); *modelled age* (95% range, a BP)	Assigned age (a BP)	Dominant taxa and characteristic features, including pollen concentrations (PC, grains/g and grains/cm^3), pollen accumulation rates (PAR, grains/cm^2/a), dominant biomes and landscape openness
MIS 3: 1038–984; *31,726/30,194–29,697/28,190*	ca. 30,700–29,000	***Artemisia*–Poaceae–Cyperaceae–*B.* sect. *Albae*** – Herbs are predominant (86–93%): *Artemisia* (24–37%), Poaceae (26–34%), and Cyperaceae (11–19%). Trees, represented by *Betula* sect. *Albae,* remain below 10%. Boreal shrubs, including *Salix, B.* sect. *Nanae/Fruticosae,* and *Alnus fruticosa* type, are at minimal (up to 3%). PC (27,000 grains/g; 27,250 grains/cm^3) and PAR (660 grains/cm^2/a) averages are relatively low. The STEP biome predominates followed by TUND. The landscape openness is high.
Last Glacial Maximum: 984–722; *29,697/28,190–18,677/17,480*	ca. 29,000–18,200	***Artemisia*–Poaceae–Cyperaceae–Ranunculaceae** – Herbaceous taxa absolutely dominate (91–98%), particularly *Artemisia* (30–53%), Poaceae (21–34%), Cyperaceae (3–17%), and Ranunculaceae (up to 12%). *Betula* sect. *Albae* diminishes to 5%, while single pollen grains of *Picea* and *Pinus sylvestris* are sporadically observed. Boreal shrubs remain at minimal levels (up to 4%), with single pollen grains of *Ericales* noticeable. PC averages decrease to 18,800 grains/g and grains/cm^3, while PAR increases to 1100 grains/cm^2/a. The STEP biome shows highest affinity scores of the entire record and the forest biome scores are minimal. The landscape becomes more open.
Lateglacial: 722–604; *18,677/17,480–13,947/12,884*	ca. 18,200–12,870	***B.* sect. *Albae*–*Artemisia*–Poaceae–*Picea* –** Proportion of arboreal pollen (8–51%) gradually increases, primarily due to a significant rise in *B.* sect. *Albae* (8–45%). *Picea* content increases from the middle part onwards, peaking at 20% in the upper part of the zone. Boreal shrubs increase steeply from 2 to 17%, predominantly represented by *Salix* (up to 11%), *Alnus fruticosa* type (up to 10%), and *B.* sect. *Nanae/Fruticosae* (up to 5%). Herbaceous taxa gradually decline from 89% to 33% towards the upper part of the zone, including *Artemisia* (13–43%), Poaceae (4–25%), and Cyperaceae (2–16%). *Thalictrum* and Rosaceae witness an increase in the upper part, up to 7% each. PC (60,000 grains/g; 52,300 grains/cm^3) and PAR (1450 grains/cm^2/a) averages increase. STEP remains the dominant biome, but TUND, CLDE and TAIG demonstrate comparably high scores, indicating mosaic vegetation and progressive afforestation of the area.
Younger Dryas: 604–558; *13,947/12,884–12,203/11,322*	ca. 12,870–11,650	***B.* sect. *Albae*–*Alnus fruticosa* type–*Artemisia*–Cyperaceae –** Pollen contribution from trees (44–61%) continues to rise, with *B.* sect. *Albae* increasing steeply from 35 to 57%. *Picea* exhibits two peaks in the lower (9%) and upper parts (12%) of the zone. Percentages of boreal shrubs increase (21–36%), with *Alnus fruticosa* type (8–18%) having the highest percentages in this zone. Contribution from herbs declines significantly to 17–20%, including *Artemisia* (5–10%), Poaceae (3–6%), Cyperaceae and *Thalictrum* (2–6%). PC (159,000 grains/g; 117,100 grains/cm^3) and PAR (3450 grains/cm^2/a) averages rapidly increase. TUND and TAIG share dominance, indicating an increased role of tree/shrub associations in the vegetation.
Early Holocene: 558–415; *12,203/11,322–8436/8095*	ca. 11,650–8280	***B.* sect. *Albae*–*Artemisia*–*Picea*–*B.* sect. *Nanae/Fruticosae* –** Proportion of arboreal pollen (66–90%) increases, primarily due to the continuous rise of *B.* sect. *Albae* (53–84%). *Picea* peaks in the lower part of the zone at 16%, followed by a decrease to 4%. *Abies*, *Pinus sylvestris* type, *Pinus sibirica* type, and *Larix* are in minimal concentrations (1–4%). Two pollen grains *of Ulmus* are found. Boreal shrubs (1–8%) decrease rapidly, including *B.* sect. *Nanae/Fruticosae* (up to 6%) and *Alnus fruticosa* type (up to 2%). Percentages of herbaceous taxa (8–32%) decrease towards the upper part of the zone, mainly represented by *Artemisia* (5–20%) and Cyperaceae (up to 5%). The highest percentages of *Pteridium* (up to 11%) are observed in this zone. PC (255,900 grains/g; 196,850 grains/cm^3) and PAR averages (8700 grains/cm^2/a) increase. A further increase in the TAIG and CLDE biome scores and a parallel decrease in the scores of TUND and STEP. Progressive afforestation of the landscape.
Middle Holocene: 415–175; *8436/8095–4525/3818*	ca. 8280–4200	***B.* sect. *Albae*–*Pinus*–*Artemisia*–Cyperaceae –** Trees dominate (84–93%), with *B.* sect. *Albae* reaching its maximum in the lower part (83%) and *Pinus sylvestris* type dominating in the upper part (57%). *Abies*, *Picea*, *Pinus sibirica* type, and *Larix* appear in small amounts. Boreal shrubs have minimal influence (up to 4%). Herbaceous taxa decrease towards the upper part of the zone from 14% to 8%, represented by *Artemisia* (2–9%), Poaceae and Cyperaceae (up to 3% each). PC (295,400 grains/g; 235,150 grains/cm^3) and PAR averages (16,000 grains/cm^2/a) reach their highest in this zone. The TAIG and CLDE biomes continue to dominate. The landscape openness progressively decreases.
Late Holocene: 175–0; *4525/3818–present*	ca. 4200– present	***Pinus*–*B.* sect. *Albae*–*Alnus fruticosa* type–*Artemisia* –** Arboreal taxa continue to dominate (80–92%) with *Pinus sylvestris* type having peaks in the lower (65%), middle (65%), and upper zones (60%) and *B.* sect. *Albae* in the lower and upper (40% each). Percentages of *Pinus sibirica* type (up to 4%), *Larix*, *Picea, Abies* are low (1–2%). The influence of boreal shrubs remains low (up to 9%), with *Alnus fruticosa* type increasing in the upper part up to 8%. Herbs, represented mainly by *Artemisia* and Poaceae, witness two peaks (14% and 11%, respectively) in the upper part of the zone. PC (213,700 grains/g; 151,350 grains/cm^3) and PAR (7200 grains/cm^2/a) averages decrease. The TAIG and CLDE biomes scores remain high and the scores of the TUND and STEP biomes stay low.

a BP (Bezrukova et al., 2022). While the length of their record (ca. 6.6–3.6 ka BP) does not allow direct comparison with the Early Holocene fire activity peaks observed in the records from the LBR and Central Yakutia, the relatively low charcoal concentrations in the Mamakan section are comparable with those in the Ochaul record.

A high-resolution macroscopic charcoal record from Lake Khamra (Fig. 1a) in Southwest Yakutia, spanning the last ca. 2200 years, reveals a phase of increased frequencies and burnt biomass accumulation between 1350 and 1050 a BP (Glückler et al., 2021). This increase corresponds to a minor peak in the longer record from Central Yakutia (Fig. 9i), but has no counterpart in the LBR records (Fig. 9j–l).

Kelly et al. (2013) concluded that recent burning of boreal forests in north-western North America exceeds the levels observed over the past 10,000 years. This conclusion has not yet been confirmed in the vast boreal zone of Siberia with its characteristic forest composition and fire regime. However, a 400-year record of changes in fire frequency in the larch-dominated northern taiga and in the pine-dominated middle taiga of Central Siberia demonstrates a well-defined maximum in the 1950s (Furyaev et al., 2001), suggesting increased anthropogenic influence. The record of Glückler et al. (2021) also shows higher fire frequency despite a shift to very low levels of charcoal accumulation in the 20th century, which they interpreted as a potential change in fire management strategies and/or a shift of the fire regime towards more frequent but smaller fires. Indeed, the fire regimes characterised by frequent and efficient ground or surface fires are usually small and do not produce much charcoal, because charred particulates are not carried into the air (Whitlock and Larsen, 2001).

Currently, a low- to moderate-intensity surface fire regime dominates the Siberian taiga, while high-intensity crown fires that are larger in size and cause much greater damage to the tree canopy predominate in the boreal forests of western Canada (De Groot et al., 2013). Based on modern observations and substantial differences in the forest composition of the two regions, Barhoumi et al. (2021) explained reconstructed changes in the Holocene charcoal records from south-western Baikal by temporal shifts from the crown fire regime (typical for spruce, fir and larch forests) to the surface fire regime characteristic of pine and birch

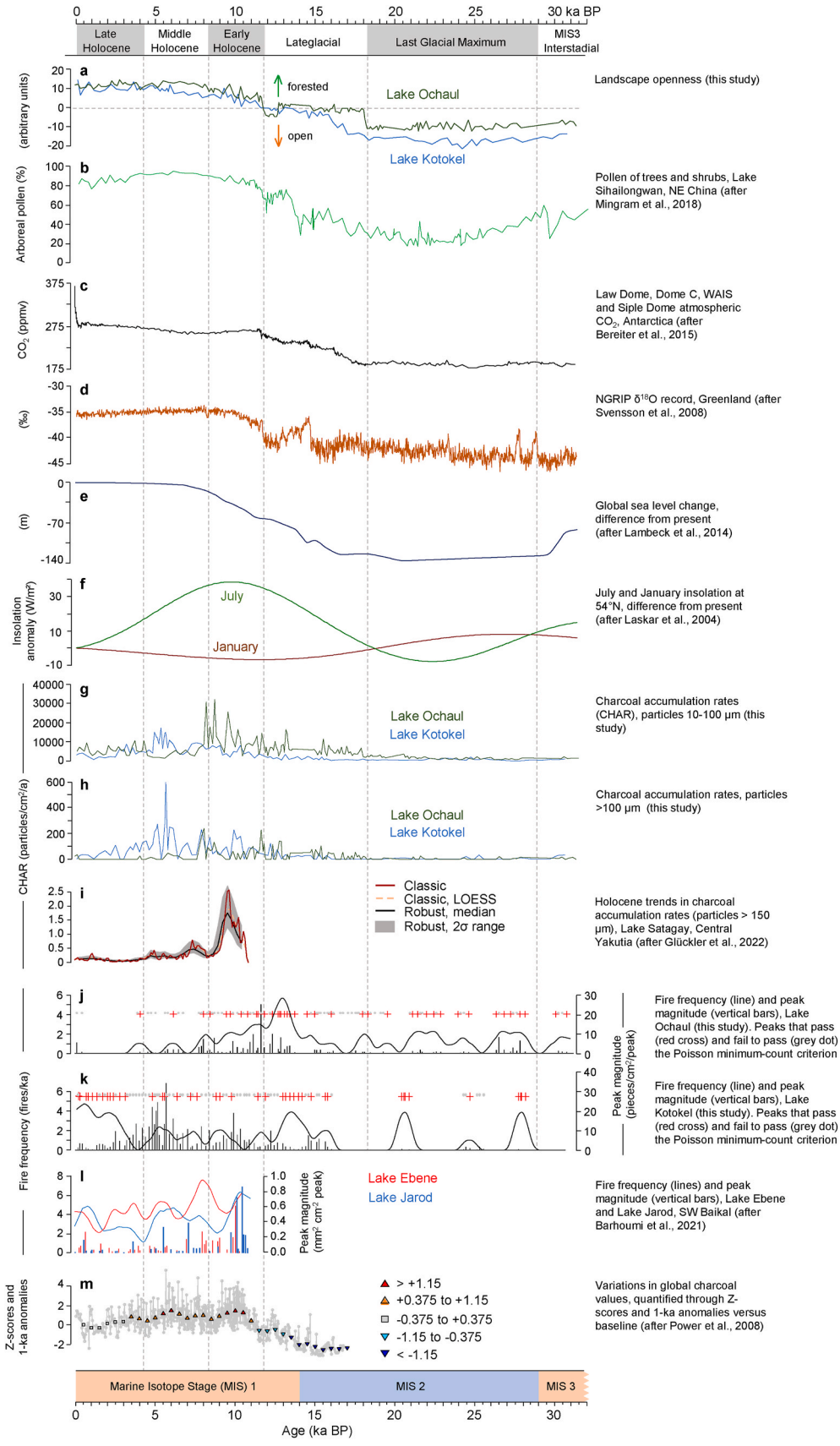

(caption on next page)

Fig. 9. Summary chart showing (a) landscape openness derived from the Och18-II and KTK19-II pollen records (this study); (b) arboreal pollen record, Lake Sihailongwan, NE China (after Mingram et al., 2018); (c) composite Law Dome, Dome C, WAIS and Siple Dome atmospheric CO_2 content (after Bereiter et al., 2015); (d) NGRIP $\delta^{18}O$ record, Greenland (after Svensson et al., 2008); (e) reconstructed changes in global sea level (after Lambeck et al., 2014); (f) mean July (red) and January (blue) insolation differences from present at 54°N (after Laskar et al., 2004); (g) charcoal accumulation rates (CHAR) for particles 10–100 μm (this study); (h) charcoal accumulation rates for particles >100 μm (this study); CHAR records from (i) Lake Satagay, Central Yakutia (after Glückler et al., 2022); (j) Lake Ochaul, Cis-Baikal and (k) Lake Kotokel, Trans-Baikal (this study): vertical bars indicate peak magnitude, red crosses and grey dots indicating peaks that meet or do not meet the Poisson minimum-count criterion, respectively, and line indicating fire frequency; (l) fire frequency (lines) and peak magnitude (vertical bars) records, Lake Ebene and Lake Jarod, SW Baikal (after Barhoumi et al., 2021); (m) variations in global charcoal data quantified through Z scores and 1000-year anomalies, defined as differences in charcoal values between the "modern" (i.e. between 1000 and 100 a BP) and the base period (after Power et al., 2008).

forests. Pollen-based reconstructions of Holocene vegetation and climate (Barhoumi et al., 2021) support this scenario, which was first proposed by Katamura et al. (2009) for Central Yakutia. The changes in the pollen and charcoal records from Ochaul and Kotokel presented here also fit into this scenario, although larch is still abundant in the forests around Lake Ochaul.

While there is general agreement on a relationship between vegetation cover and fire regime in Siberia, there are differing opinions as to whether tree species composition or vegetation structure played a more important role in driving fire dynamics. Recent macroscopic and microscopic charcoal analyses coupled with pollen and sedaDNA analyses (Glückler et al., 2022) suggest that open larch woodland correlates well with high amounts of burnt biomass during the EH, while the LH low-severity surface fire regime reflects a mediating effect of dense larch-dominated forest. The charcoal and pollen records from Ochaul and Kotokel presented here support both hypotheses and suggest that changes in the fire regime in the LBR were influenced by a combination of climatically-driven changes in vegetation composition and landscape openness.

4.2.2. *Wildfire and humans*

Although fire and climate have been shown to be powerful external factors transforming the Siberian boreal forests (Furyaev et al., 2001), the role of humans in fire activity during prehistoric and even historical periods remains understudied. For example, Kaplan et al. (2016) argued that highly mobile groups of hunter-gatherers who inhabited Europe during the last glacial were able to substantially reduce forest cover through deliberate burning. The vast territory of Siberia, including the LBR, provides evidence that large herds of herbivores likely influenced the growth and regeneration of woody plants, however, we know little to what extent this could have been caused by human activities, such as setting fires for hunting (e.g. Tarasov et al., 2021). Although anatomically modern hunter-gatherer groups have been continuously present in Cis- and Trans-Baikal since at least ca. 45–40 ka BP, their numbers and population density remained relatively small, with minor peaks around 31, 26 and 22 ka BP (Shichi et al., 2023 and references therein). While this does not preclude human contributions to the regional fire history, the available records do not allow us to confirm their direct impact. Population increased rapidly ca. 19 ka BP and was widespread by ca. 17.4 ka BP, with another peak around 14 ka BP (Fiedel and Kuzmin, 2007). The reconstructed population growth occurs concomitantly with increases in CHAR and fire activity (Fig. 9g and h), as well as pronounced shifts toward a warmer, wetter climate and a more forested landscape (Fig. 9a), making it difficult to disentangle the role of individual factors in the changing fire regime (Fig. 9j and k).

The history of Holocene hunter-gatherers in Cis-Baikal has been studied more intensively compared to other regions of Siberia (for further references see Weber, 2020). Abundant and very well-dated archaeological material indicates that Mesolithic and Early Neolithic hunter-gatherers experienced the most dramatic climatically-driven transformations of the landscape, accompanied by changes in regional fauna and flora (Tarasov et al., 2021 and references therein). These changes caused great stress (Tarasov et al., 2017), as evidenced by bioanthropological and palaeopathological studies (e.g. Lieverse, 2010; Weber, 2020), and led to changes in social organisation and subsistence strategies and stimulated many innovations, especially in hunting and fishing during the Early Neolithic Kitoi culture dated to 7560–6660 a BP (Weber, 2020). The following Middle Neolithic (ca. 6660–6050 a BP) is known as a "cultural hiatus" marked by an extreme population decline in Cis-Baikal (Weber, 2020). This decline began with the breakdown of the Kitoi culture, which took place around the time of maximum forest expansion throughout the LBR (Kobe et al., 2020). Although the region did not become completely depopulated (e.g. Kobe et al., 2022a), the lack of formal cemeteries/permanent settlements and the overall scarcity of archaeological ^{14}C dates indicate an extremely low and dispersed population (Weber, 2020). It can be speculated that the very low fire activity observed in regional charcoal records may be at least partly due to a small population size. The marked increase in fire activity in the Lake Kotokel record, which falls within the Late Neolithic phase of population recovery (Weber, 2020), provides some support to this human-fire link, although further data is required to test it.

The Late Bronze and Iron Age cultures expanded around Lake Baikal from ca. 3.5 ka BP and brought animal husbandry and other domesticates to the region (Losey and Nomokonova, 2017). The impact of the new cultures is better visible in the archaeological records of Trans-Baikal, which offers more suitable semi-open environments for husbandry and crop cultivation (Kradin et al., 2021), while the population in the northern part of the region, including the Upper Lena with Lake Ochaul, remained hunter-fisher-gatherers. Changes in the fire regime inferred from the charcoal record of Lake Kotokel (Fig. 9k) correspond to changes in subsistence economy observed in the archaeological record. However, the available charcoal records are too sparse to allow more definitive conclusions. Discussing the fire history at the southern shore of Lake Baikal, Barhoumi et al. (2021) noted that frequency of fires increased from about 1500 a BP, decreased from 900 a BP (Lake Jarod) and then stabilised from 600 a BP (Lake Ebene) onwards, which they interpreted as a phase of very recent fire management in the study area.

The above discussion shows that human influences on the fire regime are indeed difficult to prove in the study area that was inhabited by small, scattered groups of hunter-gatherers for most of the last 32 ka BP. Recently obtained ^{14}C dating of the herbivorous animal bone material from the archaeological camp site at Lake Ochaul (Fig. 2a; Kobe et al., 2022a) indicates discontinuous hunting activities going back to ca. 27,780–27,160 a BP (95.4% probability range). Other dates fall within the Mesolithic (ca. 8850–8450 a BP), the Early to Late Neolithic (ca. 6840–6510, 6490–6300 and 5720–5490 a BP) and the Iron Age (ca. 2120–1930 a BP). Kobe et al. (2022a) pointed out that the 95% probability ranges of the zooarchaeological dates correspond with minor drops in the AP percentage curve. However, a direct comparison with the charcoal record from Lake Ochaul (Fig. 6c) does not indicate a significant increase in charcoal during the archaeologically proven human presence at this site, with the exception of the Mesolithic phase, including the transition from the Early to the Middle Mesolithic (ca. 8630 a BP; Weber, 2020). The earliest evidence of small-scale farming in the Ochaul pollen record was dated to the second part of the 1st millennium BCE (Kobe et al., 2022a) and suggests distant pollen transport from Trans-Baikal, where the spread of agropastoral communities is supported by archaeological data (Kradin et al., 2021; Losey and Nomokonova, 2017) and is consistent with the reconstructed higher fire frequency around Lake Kotokel (Fig. 9k).

5. Conclusions

For the first time this paper presents a comparative high-resolution study of vegetation changes and fire histories in the Cis- and Trans-Baikal subregions covering the period from the late MIS 3 to the present. With its long-term glacial-interglacial time scale, which is rather unique for Siberia, it constitutes an important step towards a better understanding of the complicated relationships between climate change, vegetation composition and fire activity, as well as the possible influence of humans.

Together with sedaDNA analysis results it can be concluded that the low AP accumulation rates of <140 grains/cm^2/a in the Och18-II and KTK19-II records partly represent arboreal taxa that grew in refugia in both Cis- and Trans-Baikal regions during the LGM. The boreal forests of northern Europe, where *Larix* is much less common than in Siberia, cannot be used as a reference when interpreting pollen records from the latter region.

Given the robust chronologies of both pollen records, it is possible for the first time to confidently pinpoint the onset of deglaciation, which has previously been ambiguous due to poorly-constrained age-depth models of the studied sediment sequences. This occurred about three and a half millennia earlier than a prominent shift in the Greenland ice isotope records and highlights the direct influence of rising summer insolation levels on the climate and vegetation of the LBR and East Asia.

Our results show that the influence of vegetation composition and climate conditions as the main drivers of fire activity changed over time and between the two subregions. Fire activity slightly increased parallel to deglaciation throughout the LBR mainly in response to warmer conditions that led to growing availability of terrestrial biomass (mainly woody plants). By contrast, Holocene peak fire activities show a different timing, dating to the EH in Cis-Baikal and to the MH in Trans-Baikal. This spatiotemporal pattern may primarily be explained by climatically driven vegetation composition and landscape openness and the resulting difference in fire regime.

While the increasing number and quality of vegetation and climate reconstructions for the LBR allows to start discussions on the roles of both environmental factors on fire frequency and severity, we have little information about the influence of humans and large herbivores on past fire regimes. There is an urgent need to address this gap by future studies on animal and human population estimates for the study region. Palynological and bioarchaeological research in combination with geoarchaeological modelling, sedaDNA and biomarker analyses can provide the missing information.

Author contributions

AIK: Conceptualization, Methodology, Formal Analysis, Data curation, Writing – original draft, Visualization. FK: Methodology, Formal Analysis, Data curation. TL: Methodology, Visualization, Validation, Writing – Review & Editing. CL: Validation, Visualization, Writing – Review & Editing. AAS and EVB: Investigation, Data curation, Funding acquisition. JG and MW: Funding acquisition, Writing – Review & Editing. PO: Methodology, Data curation, Writing – Review & Editing. PH: Writing – Review & Editing, Supervision, PET: Conceptualization, Methodology, Writing – Review & Editing, Supervision, Funding acquisition.

Declaration of competing interest

The authors declare that they have no known competing financial interests or personal relationships that could have appeared to influence the work reported in this paper.

Data availability

Data will be made available on request.

Acknowledgements

The work of A.I. Krikunova and F. Kobe was funded by doctoral fellowships provided by the Freie Universität Berlin and the University of Alberta for the project "Individual life histories in long-term culture change: Holocene hunter-gatherers in Northern Eurasia" (Social Sciences and Humanities Research Council of Canada (SSHRC) Partnership Grant No. 895-2018-1004). This work contributes to the German Research Foundation (DFG) funded projects to J. Gliwa (GL 1048/1-1) and P.E. Tarasov (TA 540/10-1). T. Long's work was supported by the UNNC seed funding (Grant No. RESI202209004), Ningbo Science and Technology Bureau Commonweal Project (Grant No. 2022S184) and Major Humanities and Social Sciences Research Projects in Zhejiang higher education institutions (Grant No. 2023QN032). A.A. Shchetnikov and E.V. Bezrukova acknowledge financial support from the State assignment 0284-2021-0003 and the RSF grant 23-27-00022. Special thanks go to I.A. Filinov, I.O. Nechaev, M.A. Krainov, A.Y. Kazansky and G.G. Matasova for their valuable help in organising field work and lake coring, and to L.-H. Habermann and R. Arlt for assistance in laboratory work. We also thank the corresponding editor, Dr. Yan Zhao, Dr. Sebastian Breitenbach and another anonymous reviewer for their very thorough reviews and helpful comments, which were used to improve the manuscript.

References

Abraham, V., Hicks, S., Svobodová-Svitavská, H., Bozilova, E., Panajiotidis, S., Filipova-Marinova, M., Jensen, C.E., Tonkov, S., Pidek, I.A., Święta-Musznicka, J., Zimny, M., Kvavadze, E., Filbrandt-Czaja, A., Hättestrand, M., Karlıoğlu Kılıç, N., Kosenko, J., Nosova, M., Severova, E., Volkova, O., Hallsdóttir, M., Kalniņa, L., Noryśkiewicz, A. M., Noryśkiewicz, B., Pardoe, H., Christodoulou, A., Koff, T., Fontana, S.L., Alenius, T., Isaksson, E., Seppä, H., Veski, S., Pędziszewska, A., Weiser, M., Giesecke, T., 2021. Patterns in recent and Holocene pollen accumulation rates across Europe – the Pollen Monitoring Programme Database as a tool for vegetation reconstruction. Biogeosciences 18 (15), 4511–4534. https://doi.org/10.5194/bg-18-4511-2021.

Alpat'ev, A.M., Arkhangel'skii, A.M., Podoplelov, N.Y., Stepanov, A.Y., 1976. Physical Geography of the USSR (The Asian Part). Vysshaya Shkola, Moscow (in Russian).

Andreev, A.A., Tarasov, P.E., 2013. Northern Asia. In: Elias, S.A. (Ed.), The Encyclopedia of Quaternary Science, vol. 4. Elsevier, Amsterdam, pp. 164–172.

Andreev, A.A., Tarasov, P.E., Klimanov, V.A., Melles, M., Lisitsyna, O.M., Hubberten, H.-W., 2004. Vegetation and climate changes around the Lama Lake, Taymyr Peninsula, Russia during the late Pleistocene and Holocene. Quat. Int. 122, 69–84. https://doi.org/10.1016/j.quaint.2004.01.032.

Barhoumi, C., Peyron, O., Joannin, S., Subetto, D., Kryshen, A., Drobyshev, I., Girardin, M.P., Brossier, B., Paradis, L., Pastor, T., Alleaume, S., Ali, A.A., 2019. Gradually increasing forest fire activity during the Holocene in the northern Ural region (Komi Republic, Russia). Holocene 29, 1906–1920. https://doi.org/10.1177/0959683619865593.

Barhoumi, C., Ali, A.A., Peyron, O., Dugerdil, L., Borisova, O., Golubeva, Y., Subetto, D., Kryshen, A., Drobyshev, I., Ryzhkova, N., Joannin, S., 2020. Did long-term fire control the coniferous boreal forest composition of the northern Ural region (Komi Republic, Russia)? J. Biogeogr. 47, 2426–2441. https://doi.org/10.1111/jbi.13922.

Barhoumi, C., Vogel, M., Dugerdil, L., Limani, H., Joannin, S., Peyron, O., Ali, A.A., 2021. Holocene fire regime changes in the southern Lake Baikal region influenced by climate-vegetation-anthropogenic activity interactions. Forests 12, 978. https://doi.org/10.3390/f12080978.

Barrett, C.M., Kelly, R., Higuera, P.E., Hu, F.S., 2013. Climatic and land cover influences on the spatiotemporal dynamics of Holocene boreal fire regimes. Ecology 94, 389–402. https://doi.org/10.1890/12-0840.1.

Belov, A.V., Ljamkin, V.F., Sokolova, L.P., 2002. Cartographic Study of Biota. Oblmashinform, Irkutsk (in Russian).

Bereiter, B., Eggleston, S., Schmitt, J., Nehrbass-Ahles, C., Stocker, T.F., Fischer, H., Kipfstuhl, S., Chappellaz, J., 2015. Revision of the EPICA Dome C CO_2 record from 800 to 600 kyr before present. Geophys. Res. Lett. 42, 542–549. https://doi.org/10.1002/2014GL061957.

Beug, H.-J., 2004. Leitfaden der Pollenbestimmung: für Mitteleuropa und angrenzende Gebiete. Pfeil, München.

Bezrukova, E.V., Abzaeva, A.A., Letunova, P.P., Kulagina, N.V., Vershinin, K.E., Belov, A. V., Orlova, L.A., Danko, L.V., Krapivina, S.M., 2005. Post-glacial history of Siberian spruce (*Picea obovata*) in the Lake Baikal area and the significance of this species as a paleo-environmental indicator. Quat. Int. 136, 47–57. https://doi.org/10.1016/j.quaint.2004.11.007.

Bezrukova, E.V., Abzaeva, A.A., Letunova, P.P., Kulagina, N.V., Orlova, L.A., 2009. Evidence of environmental instability of the Lake Baikal area after the last glaciation (based on pollen records from peatlands). Archaeol. Ethnol. Anthropol. Eurasia 37, 17–25. https://doi.org/10.1016/j.aeae.2009.11.002.

Bezrukova, E.V., Tarasov, P.E., Solovieva, N., Krivonogov, S.K., Riedel, F., 2010. Last glacial–interglacial vegetation and environmental dynamics in southern Siberia: chronology, forcing and feedbacks. Palaeogeogr. Palaeoclimatol. Palaeoecol. 296, 185–198. https://doi.org/10.1016/j.palaeo.2010.07.020.

Bezrukova, E.V., Hildebrandt, S., Letunova, P.P., Ivanov, E.V., Orlova, L.A., Müller, S., Tarasov, P.E., 2013. Vegetation dynamics around Lake Baikal since the middle Holocene reconstructed from the pollen and botanical composition analyses of peat sediments and its implication for paleoclimatic and archeological research. Quat. Int. 290–291, 35–45. https://doi.org/10.1016/j.quaint.2012.10.043.

Bezrukova, E.V., Reshetova, S.A., Tetenkin, A.V., Tarasov, P.E., Leipe, C., 2022. The Early Neolithic–Middle Bronze age environmental history of the Mamakan archaeological area, Eastern Siberia. Quat. Int. 623, 159–168. https://doi.org/10.1016/j.quaint.2021.12.006.

Bilgaev, A., Dong, S., Li, F., Cheng, H., Tulohonov, A., Sadykova, E., Mikheeva, A., 2021. Baikal region (Russia) development prospects based on the green economy principles. Sustainability 13, 157. https://doi.org/10.3390/su13010157.

Binney, H., Edwards, M., Macias-Fauria, M., Lozhkin, A., Anderson, P., Kaplan, J.O., Andreev, A., Bezrukova, E., Blyakharchuk, T., Jankovska, V., Khazina, I., Krivonogov, S., Kremenetski, K., Nield, J., Novenko, E., Ryabogina, N., Solovieva, N., Willis, K., Zernitskaya, V., 2017. Vegetation of Eurasia from the last glacial maximum to present: key biogeographic patterns. Quat. Sci. Rev. 157, 80–97. https://doi.org/10.1016/j.quascirev.2016.11.022.

Blaauw, M., Christen, J.A., 2011. Flexible paleoclimate age-depth models using an autoregressive gamma process. Bayesian Analysis 6, 457–474. https://doi.org/10.1214/ba/1339616472.

Blarquez, O., Ali, A.A., Girardin, M.P., Grondin, P., Fréchette, B., Bergeron, Y., Hély, C., 2015. Regional paleofire regimes affected by non-uniform climate, vegetation and human drivers. Sci. Rep. 5, 13356 https://doi.org/10.1038/srep13356.

Boyarkin, V.M., 2007. Geografiya Irkutskoi Oblasti. Publishing Hous Sarma, Irkutsk (in Russian).

Bronk Ramsey, C., 1995. Radiocarbon calibration and analysis of stratigraphy: the OxCal program. Radiocarbon 37, 425–430. https://doi.org/10.1017/S0033822200030903.

Brossier, B., Oris, F., Finsinger, W., Asselin, H., Bergeron, Y., Ali, A.A., 2014. Using tree-ring records to calibrate peak detection in fire reconstructions based on sedimentary charcoal records. Holocene 24 (6), 635–645. https://doi.org/10.1177/0959683614526902.

Carcaillet, C., Bergeron, Y., Richard, P.J., Fréchette, B., Gauthier, S., Prairie, Y.T., 2001. Change of fire frequency in the eastern Canadian boreal forests during the Holocene: does vegetation composition or climate trigger the fire regime? J. Ecol. 89, 930–946. https://doi.org/10.1111/j.1365-2745.2001.00614.x.

Cheng, H., Zhang, H., Spötl, C., Baker, J., Sinha, Li, A.H., Bartolomé, M., Moreno, A., Kathayat, G., Zhao, J., Dong, X., Li, Y., Ning, Y., Jia, X., Zong, B., Brahim, Y.A., Pérez-Mejiás, C., Cai, Y., Novello, V.F., Cruz, F.W., Severinghausi, J.P., An, Z., Edwards, R.L., 2020. Timing and structure of the Younger Dryas event and its underlying climate dynamics. Proc. Natl. Acad. Sci. USA 117, 23408–23417. https://www.pnas.org/cgi/doi/10.1073/pnas.2007869117.

Chevalier, M., Dallmeyer, A., Weitzel, N., Li, C., Baudouin, J.-P., Herzschuh, U., Cao, X., Hense, A., 2023. Refining data–data and data–model vegetation comparisons using the Earth mover's distance (EMD). Clim. Past 19, 1043–1060. https://doi.org/10.5194/cp-19-1043-2023.

Chipman, M.L., Hudspith, V., Higuera, P.E., Duffy, P.A., Kelly, R., Oswald, W.W., Hu, F. S., 2015. Spatiotemporal patterns of tundra fires: late-Quaternary charcoal records from Alaska. Biogeosciences 12 (13), 4017–4027. https://doi.org/10.5194/bg-12-4017-2015.

Chlachula, J., 2017. Chronology and environments of the Pleistocene peopling of North Asia. Archaeol. Res. Asia 12, 33–53. https://doi.org/10.1016/j.ara.2017.07.006.

Clark, J.S., 1988a. Stratigraphic charcoal analysis on petrographic thin sections: application to fire history in northwestern Minnesota. Quat. Res. 30, 81–91. https://doi.org/10.1016/0033-5894(88)90089-0.

Clark, J.S., 1988b. Particle motion and the theory of charcoal analysis: source area, transport, deposition, and sampling. Quat. Res. 30, 67–80. https://doi.org/10.1016/0033-5894(88)90088-9.

Clark, J.S., Lynch, J., Stocks, B.J., Goldammer, J.G., 1998. Relationships between charcoal particles in air and sediments in west-central Siberia. Holocene 8, 19–29. https://doi.org/10.1191/095968398672501165.

Clear, J.L., Molinari, C., Bradshaw, R.H.W., 2014. Holocene fire in Fennoscandia and Denmark. Int. J. Wildland Fire 23 (6), 781–789. https://doi.org/10.1071/WF13188.

DeFries, R.S., Hansen, M.C., Townshend, J.R., Janetos, A.C., Loveland, T.R., 2000. A new global 1-km dataset of percentage tree cover derived from remote sensing. Global Change Biol. 6 (2), 247–254. https://doi.org/10.1046/j.1365-2486.2000.00296.x.

De Groot, W.J., Cantin, A.S., Flannigan, M., Soja, A.J., Gowman, L.M., Newbery, A., 2013. A comparison of Canadian and Russian boreal forest fire regimes. For. Ecol. Manag. 294, 23–34. https://doi.org/10.1016/j.foreco.2012.07.033.

Demske, D., Heumann, G., Granoszewski, W., Nita, M., Mamakowa, K., Tarasov, P., Oberhänsli, H., 2005. Late glacial and Holocene vegetation and regional climate variability evidenced in high-resolution pollen records from Lake Baikal. Global Planet. Change 46, 255–279. https://doi.org/10.1016/j.gloplacha.2004.09.020.

Dixon, R., 2021. Siberia's wildfires are bigger than all the world's other blazes combined. Wash. Post. August 11, 2021 at 8:08 a.m. EDT. https://www.washingtonpost.com/world/2021/08/11/siberia-fires-russia-climate/. accessed in April 2024.

Dolukhanov, P.M., Shukurov, A.M., Tarasov, P.E., Zaitseva, G.I., 2002. Colonization of northern Eurasia by modern humans: radiocarbon chronology and environment. J. Archaeol. Sci. 29, 593–606. https://doi.org/10.1006/jasc.2001.0753.

Duffin, K.I., Gillson, L., Willis, K.J., 2008. Testing the sensitivity of charcoal as an indicator of fire events in savanna environments: quantitative predictions of fire proximity, area and intensity. Holocene 18, 279–291. https://doi.org/10.1177/0959683607086766.

Edwards, M.E., Anderson, P.M., Brubaker, L.B., Ager, T.A., Andreev, A.A., Bigelow, N.H., Cwynar, L.C., Eisner, W.R., Harrison, S.P., Hu, F.-S., Jolly, D., Lozhkin, A.V., MacDonald, G.M., Mock, C.J., Ritchie, J.C., Sher, A.V., Spear, R.W., Yu, G., 2000. Pollen-based biomes for Beringia 18,000, 6000 and 0 14C yr bp. J. Biogeogr. 27, 521–554. https://doi.org/10.1046/j.1365-2699.2000.00426.x.

Eichler, A., Tinner, W., Brütsch, S., Olivier, S., Papina, T., Schwikowski, M., 2011. An ice-core based history of Siberian forest fires since AD 1250. Quat. Sci. Rev. 30, 1027–1034. https://doi.org/10.1016/j.quascirev.2011.02.007.

Fedotov, A.P., Vorobyeva, S.S., Vershinin, K.E., Nurgaliev, D.K., Enushchenko, I.V., Krapivina, S.M., Tarakanova, K.V., Ziborova, G.A., Yassonov, P.G., Borissov, A.S., 2012. Climate changes in East Siberia (Russia) in the Holocene based on diatom, chironomid and pollen records from the sediments of Lake Kotokel. J. Paleolimnol. 47, 617–630. https://doi.org/10.1007/s10933-012-9586-5.

Fiedel, S.J., Kuzmin, Y.V., 2007. Radiocarbon date frequency as an index of intensity of Paleolithic occupation of Siberia: did humans react predictably to climate oscillations? Radiocarbon 49 (2), 741–756. https://doi.org/10.1017/S0033822200042624.

Furyaev, V.V., Vaganov, E.A., Tchebakova, N.M., Valendik, E.N., 2001. Effects of fire and climate on successions and structural changes in the Siberian boreal forest. Eurasian J. For. Res. 2, 1–15.

Galaziy, G.I., 1993. Baikal atlas. In: Federalnaya Sluzhba Geodezii I Kartografii Rossii. Moscow (in Russian).

Glückler, R., Herzschuh, U., Kruse, S., Andreev, A., Vyse, S.A., Winkler, B., Biskaborn, B. K., Pestrykova, L., Dietze, E., 2021. Wildfire history of the boreal forest of southwestern Yakutia (Siberia) over the last two millennia documented by a lake-sedimentary charcoal record. Biogeosciences 18, 4185–4209. https://doi.org/10.5194/bg-18-4185-2021.

Glückler, R., Geng, R., Grimm, L., Baisheva, I., Herzschuh, U., Stoof-Leichsenring, K.R., Kruse, S., Andreev, A., Pestryakova, L., Dietze, E., 2022. Holocene wildfire and vegetation dynamics in Central Yakutia, Siberia, reconstructed from lake-sediment proxies. Front. Ecol. Evol. 10, 962906 https://doi.org/10.3389/fevo.2022.962906.

Goldammer, J.G., Furyaev, V.V., 1996. Fire in Ecosystems of Boreal Eurasia. Springer, Dordrecht, Netherlands.

Grimm, E.C., 2011. Tilia 1.7.16 Software. Illinois State Museum, Research and Collection Center, Springfield, IL.

Halofsky, J.E., Peterson, D.L., Harvey, B.J., 2020. Changing wildfire, changing forests: the effects of climate change on fire regimes and vegetation in the Pacific Northwest, USA. Fire Ecol. 16, 4. https://doi.org/10.1186/s42408-019-0062-8.

Hély, C., Girardin, M.P., Ali, A.A., Carcaillet, C., Brewer, S., Bergeron, Y., 2010. Eastern boreal North American wildfire risk of the past 7000 years: a model-data comparison. Geophys. Res. Lett. 37, L14709 https://doi.org/10.1029/2010GL043706.

Herzschuh, U., 2020. Legacy of the Last Glacial on the present-day distribution of deciduous versus evergreen boreal forests. Global Ecol. Biogeogr. 29, 198–206. https://doi.org/10.1111/geb.13018.

Herzschuh, U., Böhmer, T., Chevalier, M., Dallmeyer, A., Li, C., Cao, X., Hébert, R., Peyron, O., Nazarova, L., Novenko, E.Y., Park, J., Rudaya, N.A., Schlütz, F., Shumilovskikh, L.S., Tarasov, P.E., Wang, Y., Wen, R., Xu, Q., Zheng, Z., 2023. Regional pollen-based Holocene temperature and precipitation patterns depart from the Northern Hemisphere mean trends. Clim. Past 19, 1481–1506. https://doi.org/10.5194/cp-19-1481-2023.

Higuera, P.E., Brubaker, L.B., Anderson, P.M., Hu, F.S., Brown, T.A., 2009. Vegetation mediated the impacts of postglacial climate change on fire regimes in the south-central Brooks Range, Alaska. Ecol. Monogr. 79 (2), 201–219. https://doi.org/10.1890/07-2019.1.

Higuera, P.E., Chipman, M.L., Barnes, J.L., Urban, M.A., Hu, F.S., 2011. Variability of tundra fire regimes in Arctic Alaska: millennial-scale patterns and ecological implications. Ecol. Appl. 21 (8), 3211–3226. https://doi.org/10.1890/11-0387.1.

Ivy-Ochs, S., Monegato, G., Reitner, J.M., 2023. Chapter 20 - The Alps: glacial landforms during the deglaciation (18.9–14.6 ka). In: Palacios, D., Hughes, P.D., García-Ruiz, J. M., Andrés, N. (Eds.), European Glacial Landscapes. Elsevier, Amsterdam, pp. 175–183. https://doi.org/10.1016/B978-0-323-91899-2.00005-X.

Jackson, M.S., Kelly, M.A., Russell, J.M., Doughty, A.M., Howley, J.A., Chipman, J.W., Cavagnaro, D., Nakileza, B., Zimmerman, S.R.H., 2019. High-latitude warming initiated the onset of the last deglaciation in the tropics. Sci. Adv. 5, eaaw2610. https://www.science.org/doi/10.1126/sciadv.aaw2610.

Jarvis, A., Reuter, H.I., Nelson, A., Guevara, E., 2008. Hole-filled SRTM for the globe version 4. CGIAR-CSI SRTM 90 m Database. https://srtm.csi.cgiar.org.

Kageyama, M., Peyron, O., Pinot, S., Tarasov, P., Guiot, J., Joussaume, S., Ramstein, G., 2001. The Last Glacial Maximum climate over Europe and western Siberia: a PMIP comparison between models and data. Clim. Dynam. 17, 23–43. https://doi.org/10.1007/s003820000095.

Kaplan, J.O., Pfeiffer, M., Kolen, J.C., Davis, B.A., 2016. Large scale anthropogenic reduction of forest cover in Last Glacial Maximum Europe. PLoS One 11 (11), e0166726. https://doi.org/10.1371/journal.pone.0166726.

Katamura, F., Fukuda, M., Bosikov, N.P., Desyatkin, R.V., 2009. Charcoal records from thermokarst deposits in central Yakutia, eastern Siberia: implications for forest fire history and thermokarst development. Quat. Res. 71, 36–40. https://doi.org/10.1016/j.yqres.2008.08.003.

Kelly, R., Chipman, M.L., Higuera, P.E., Stephanova, V., Brubaker, L., Hu, F.S., 2013. Recent burning of boreal forests exceeds fire regime limits of the past 10,000 years. Proc. Natl. Acad. Sci. 110 (32), 13055–13060. https://doi.org/10.1073/pnas.1305069110.

Khenzykhenova, F., Lipnina, E., Danukalova, G., Shchetnikov, A., Osipova, E., Semenei, E., Tumurov, E., Lokhov, D., 2019. The area surrounding the world-famous geoarchaeological site Mal'ta (Baikal Siberia): new data on the chronology, archaeology, and fauna. Quat. Int. 509, 17–29. https://doi.org/10.1016/j.quaint.2018.02.026.

Knight, C.A., Battles, J.J., Bunting, M.J., Champagne, M., Wanket, J.A., Wahl, D.B., 2022. Methods for robust estimates of tree biomass from pollen accumulation rates: quantifying paleoecological reconstruction uncertainty. Front. Ecol. Evol. 10, 956143 https://doi.org/10.3389/fevo.2022.956143.

Kobe, F., Bezrukova, E.V., Leipe, C., Shchetnikov, A.A., Goslar, T., Wagner, M., Kostrova, S.S., Tarasov, P.E., 2020. Holocene vegetation and climate history in Baikal Siberia reconstructed from pollen records and its implications for archaeology. Archaeol. Res. Asia 23, 100209. https://doi.org/10.1016/j.ara.2020.100209.

Kobe, F., Hoelzmann, P., Gliwa, J., Olschewski, P., Peskov, S.A., Shchetnikov, A.A., Danukalova, G.A., Osipova, E.M., Goslar, T., Leipe, C., Wagner, M., Bezrukova, E.V., Tarasov, P.E., 2022a. Lateglacial–Holocene environments and human occupation in the Upper Lena region of Eastern Siberia derived from sedimentary and zooarchaeological data from Lake Ochaul. Quat. Int. 623, 139–158. https://doi.org/10.1016/j.quaint.2021.09.019.

Kobe, F., Leipe, C., Shchetnikov, A.A., Hoelzmann, P., Gliwa, J., Olschewski, P., Goslar, T., Wagner, M., Bezrukova, E.V., Tarasov, P.E., 2022b. Not herbs and forbs alone: pollen-based evidence for the presence of boreal trees and shrubs in Cis-Baikal (Eastern Siberia) derived from the Last Glacial Maximum sediment of Lake Ochaul. J. Quat. Sci. 37, 868–883. https://doi.org/10.1002/jqs.3290.

Korsakova, O., Vashkov, A., Nosova, O., 2023. Chapter 12 - European Russia: glacial landforms during deglaciation. In: Palacios, D., Hughes, P.D., García-Ruiz, J.M., Andrés, N. (Eds.), European Glacial Landscapes. Elsevier, Amsterdam, pp. 105–110. https://doi.org/10.1016/B978-0-323-91899-2.00025-5.

Kostrova, S.S., Meyer, H., Chapligin, B., Kossler, A., Bezrukova, E.V., Tarasov, P.E., 2013. Holocene oxygen isotope record of diatoms from Lake Kotokel (southern Siberia, Russia) and its palaeoclimatic implications. Quat. Int. 290–291, 21–34. https://doi.org/10.1016/j.quaint.2012.05.011.

Kostrova, S.S., Meyer, H., Fernandoy, F., Werner, M., Tarasov, P.E., 2020. Moisture origin and stable isotope characteristics of precipitation in southeast Siberia. Hydrol. Process. 34, 51–67. https://doi.org/10.1002/hyp.13571.

Kradin, N.N., Khubanova, A.M., Bazarov, B.A., Miyagashev, D.A., Khubanov, V.B., Konovalov, P.B., Klementiev, A.M., Posokhov, V.F., Ventresca Miller, A.R., 2021. Iron age societies of Western Transbaikalia: reconstruction of diet and lifeways. J. Archaeol. Sci. Rep 38, 102973. https://doi.org/10.1016/j.jasrep.2021.102973.

Lambeck, K., Rouby, H., Purcell, A., Sun, Y., Sambridge, M., 2014. Sea level and global ice volumes from the last glacial maximum to the Holocene. Proc. Natl. Acad. Sci. USA 111, 15296–15303. https://doi.org/10.1073/pnas.1411762111.

Lamentowicz, M., Słowiński, M., Marcisz, K., Zielińska, M., Kaliszan, K., Lapshina, E., Gilbert, D., Buttler, A., Fiałkiewicz-kozieł, B., Jassey, V., Laggoun-Défarge, F., Kołaczek, P., 2015. Hydrological dynamics and fire history of the last 1300 years in western Siberia reconstructed from a high-resolution, ombrotrophic peat archive. Quat. Res. 84, 312–325. https://doi.org/10.1016/j.yqres.2015.09.002.

Lankia, H., Wallenius, T., Várkonyi, G., Kouki, J., Snäll, T., 2012. Forest fire history, aspen and goat willow in a Fennoscandian old-growth landscape: are current population structures a legacy of historical fires? J. Veg. Sci. 23, 1159–1169. https://doi.org/10.1111/j.1654-1103.2012.01426.x.

Laskar, J., Robutel, P., Joutel, F., Gastineau, M., Correia, A.C.M., Levrard, B., 2004. A long-term numerical solution for the insolation quantities of the Earth. Astron. Astrophys. 428, 261–285. https://doi.org/10.1051/0004-6361:20041335.

Lbova, L.V., 2009. Chronology and paleoecology of the early Upper Paleolithic in the Transbaikal region (Siberia). Eurasian Prehistory 5, 109–114.

Leipe, C., Kobe, F., Müller, S., 2019. Testing the performance of sodium polytungstate and peat sediment samples. Quat. Int. 516, 207–214. https://doi.org/10.1016/j.quaint.2018.01.029.

Lieverse, A.R., 2010. Health and behavior in mid-Holocene Cis-Baikal: biological indicators of adaptation and cultural change. In: Weber, A.W., Katzenberg, M.A., Schurr, T. (Eds.), Prehistoric Hunter–Gatherers of the Baikal Region, Siberia: Bioarchaeological Studies of Past Life Ways. University of Pennsylvania Press, Philadelphia, pp. 135–173.

Lisiecki, L.E., Raymo, M.E., 2005. A Pliocene-Pleistocene stack of 57 globally distributed benthic $\delta^{18}O$ records. Paleoceanography 20, PA1003. https://doi.org/10.1029/2004PA001071.

Litt, T., Stebich, M., 1999. Bio- and chronostratigraphy of the lateglacial in the Eifel region, Germany. Quat. Int. 61, 5–16. https://doi.org/10.1016/S1040-6182(99)00013-0.

Litt, T., Brauer, A., Goslar, T., Merkt, J., Bałaga, K., Mueller, H., Ralska-Jasiewiczowa, M., Stebich, M., Negendank, J.F., 2001. Correlation and synchronisation of Lateglacial continental sequences in northern Central Europe based on annually laminated lacustrine sediments. Quat. Sci. Rev. 20, 1233–1249. https://doi.org/10.1016/S0277-3791(00)00149-9.

Losey, R.J., Nomokonova, T. (Eds.), 2017. Holocene Zooarchaeology of Cis-Baikal. Archaeology in China and East Asia 6. Nünnerich–Asmus Verlag & Media GmbH, Mainz.

MacDonald, G.M., Larsen, C.P., Szeicz, J.M., Moser, K.A., 1991. The reconstruction of boreal forest fire history from lake sediments: a comparison of charcoal, pollen, sedimentological, and geochemical indices. Quat. Sci. Rev. 10, 53–71. https://doi.org/10.1016/0277-3791(91)90030-X.

Mackay, A.W., Bezrukova, E.V., Boyle, J.F., Holmes, J.A., Panizzo, V.N., Piotrowska, N., Shchetnikov, A., Shilland, E.M., Tarasov, P., White, D., 2013. Multiproxy evidence for abrupt climate change impacts on terrestrial and freshwater ecosystems in the Ol'khon region of Lake Baikal, central Asia. Quat. Int. 290–291, 46–56. https://doi.org/10.1016/j.quaint.2012.09.031.

Magne, G., Brossier, B., Gandouin, E., Paradis, L., Drobyshev, I., Kryshen, A., Hély, C., Alleaume, S., Ali, A., 2019. Lacustrine charcoal peaks provide an accurate record of surface wildfires in a North European boreal forest. Holocene 30, 380–388. https://doi.org/10.1177/0959683619887421.

Markova, A.K., Puzachenko, A.Yu, van Kolfschoten, T., Kosintsev, P.A., Kuznetsova, T.V., Tikhonov, A.N., Bachura, O.P., Ponomarev, D.V., van der Plicht, J., Kuitems, M., 2015. Changes in the Eurasian distribution of the musk ox (*Ovibos moschatus*) and the extinct bison (*Bison priscus*) during the last 50 ka BP. Quat. Int. 378, 99–110. https://doi.org/10.1016/j.quaint.2015.01.020.

Marshall, J.A., Roering, J.J., Gavin, D.G., Granger, D.E., 2017. Late Quaternary climatic controls on erosion rates and geomorphic processes in western Oregon, USA. GSA Bulletin 129, 715–731. https://doi.org/10.1130/B31509.1.

Mingram, J., Stebich, M., Schettler, G., Hu, Y., Rioual, P., Nowaczyk, N., Dulski, P., You, H., Opitz, S., Liu, Q., Liu, J., 2018. Millennial-scale East Asian monsoon variability of the last glacial deduced from annually laminated sediments from Lake Sihailongwan, N.E. China. Quat. Sci. Rev. 201, 57–76. https://doi.org/10.1016/j.quascirev.2018.09.023.

Mokhova, L., Tarasov, P., Bazarova, V., Klimin, M., 2009. Quantitative biome reconstruction using modern and late Quaternary pollen data from the southern part of the Russian Far East. Quat. Sci. Rev. 28, 2913–2926. https://doi.org/10.1016/j.quascirev.2009.07.018.

Müller, S., Tarasov, P.E., Andreev, A.A., Tütken, T., Gartz, S., Diekmann, B., 2010. Late Quaternary vegetation and environments in the Verkhoyansk Mountains region (NE Asia) reconstructed from a 50-kyr fossil pollen record from Lake Billyakh. Quat. Sci. Rev. 29, 2071–2086. https://doi.org/10.1016/j.quascirev.2010.04.024.

Müller, S., Tarasov, P.E., Hoelzmann, P., Bezrukova, E.V., Kossler, A., Krivonogov, S.K., 2014. Stable vegetation and environmental conditions during the Last Glacial Maximum: new results from Lake Kotokel (Lake Baikal region, southern Siberia, Russia). Quat. Int. 348, 14–24. https://doi.org/10.1016/j.quaint.2013.12.012.

Nakagawa, T., Tarasov, P., Staff, R., Bronk Ramsey, C., Marshall, M., Schlolaut, G., Bryant, C., Brauer, A., Lamb, H., Haraguchi, T., Gotanda, K., Kitaba, I., Kitagawa, H., van der Plicht, J., Yonenobu, H., Omori, T., Yokoyama, Y., Tada, R., Yasuda, Y., Suigetsu 2006 Project Members, 2021. The spatio-temporal structure of the Lateglacial to early Holocene transition reconstructed from the pollen record of Lake Suigetsu and its precise correlation with other key global archives: implications for palaeoclimatology and archaeology. Global Planet. Change 202, 103493. https://doi.org/10.1016/j.gloplacha.2021.103493.

Ohlson, M., Tryterud, E., 2000. Interpretation of the charcoal record in forest soils: forest fires and their production and deposition of macroscopic charcoal. Holocene 10 (4), 519–525. https://doi.org/10.1191/095968300667442551.

Osipov, E.Y., Khlystov, O.M., 2010. Glaciers and meltwater flux to Lake Baikal during the Last Glacial Maximum. Palaeogeogr. Palaeoclimatol. Palaeoecol. 294, 4–15. https://doi:10.1016/j.palaeo.2010.01.031.

Osipov, E.Y., Grachev, M.A., Mats, V.D., Khlystov, O.M., Breitenbach, S., 2003. Mountain glaciers of the Pleistocene Last Glacial Maximum in the northwestern Barguzin Range (northern Baikal Region): paleoglacial reconstruction. Russ. Geol. Geophys. 44 (7), 652–663.

Petit, R.J., Hu, F.S., Dick, C.W., 2008. Forests of the past: a window to future changes. Science 320, 1450–1452.

Power, M.J., Marlon, J., Ortiz, N., Bartlein, P.J., Harrison, S.P., Mayle, F.E., Ballouche, A., Bradshaw, R.H.W., Carcaillet, C., Cordova, C., Mooney, S., Moreno, P. I., Prentice, I.C., Thonicke, K., Tinner, W., Whitlock, C., Zhang, Y., Zhao, Y., Ali, A.A., Anderson, R.S., Beer, R., Behling, H., Briles, C., Brown, K.J., Brunelle, A., Bush, M., Camill, P., Chu, G.Q., Clark, J., Colombaroli, D., Connor, S., Daniau, A.-L., Daniels, M., Dodson, J., Doughty, E., Edwards, M.E., Finsinger, W., Foster, D., Frechette, J., Gaillard, M.-J., Gavin, D.G., Gobet, E., Haberle, S., Hallett, D.J., Higuera, P., Hope, G., Horn, S., Inoue, J., Kaltenrieder, P., Kennedy, L., Kong, Z.C., Larsen, C., Long, C.J., Lynch, J., Lynch, E.A., McGlone, M., Meeks, S., Mensing, S., Meyer, G., Minckley, T., Mohr, J., Nelson, D.M., New, J., Newnham, R., Noti, R., Oswald, W., Pierce, J., Richard, P.J.H., Rowe, C., Sanchez Goñi, M.F., Shuman, B.N., Takahara, H., Toney, J., Turney, C., Urrego-Sanchez, D.H., Umbanhowar, C., Vandergoes, M., Vanniere, B., Vescovi, E., Walsh, M., Wang, X., Williams, N., Wilmshurst, J., Zhang, J.H., 2008. Changes in fire regimes since the Last Glacial Maximum: an assessment based on a global synthesis and analysis of charcoal data. Clim. Dynam. 30, 887–907. https://doi.org/10.1007/s00382-007-0334-x.

Power, M.J., Marlon, J.R., Bartlein, P.J., Harrison, S.P., 2010. Fire history and the Global Charcoal Database: a new tool for hypothesis testing and data exploration. Palaeogeogr. Palaeoclimatol. Palaeoecol. 291, 52–59. https://doi.org/10.1016/j.palaeo.2009.09.014.

Prentice, I.C., Webb III, T., 1998. Biome 6000: reconstructing global mid-Holocene vegetation patterns from palaeoecological records. J. Biogeogr. 25, 997–1005. https://www.jstor.org/stable/2846196.

Prentice, I.C., Cramer, W., Harrison, S.P., Leemans, R., Monserud, R.A., Solomon, A.M., 1992. A global biome model based on plant physiology and dominance, soil properties and climate. J. Biogeogr. 19, 117–134. https://doi.org/10.2307/2845499.

Prentice, I.C., Guiot, J., Huntley, B., Jolly, D., Cheddadi, R., 1996. Reconstructing biomes from palaeoecological data: a general method and its application to European pollen data at 0 and 6 ka. Clim. Dynam. 12, 185–194. https://doi.org/10.1007/BF00211617.

Puzachenko, A.Yu, Markova, A.K., Kosintsev, P.A., van Kolfschoten, T., van der Plicht, J., Kuznetsova, T.V., Tikhonov, A.N., Ponomarev, D.V., Kuitems, M., Bachura, O.P., 2017. The Eurasian mammoth distribution during the second half of the Late

Pleistocene and the Holocene: regional aspects. Quat. Int. 445, 71–88. https://doi.org/10.1016/j.quaint.2016.05.019.
R Core Team, 2016. R: A Language and Environment for Statistical Computing. R Foundation for Statistical Computing, Vienna, Austria.
Reille, M., 1992. Pollen et Spores d'Europe et d'Afrique du Nord. Laboratoire de Botanique Historique et Palynologie. URA CNRS, Marseille, France.
Reille, M., 1995. Pollen et Spores d'Europe et d'Afrique du Nord. Supplement 1. Laboratoire de Botanique Hislorique el Palynologie. URA CNRS, Marseille, France.
Reille, M., 1998. Pollen et Spores d'Europe et d'Afrique du Nord, vol. 2. Laboratoire de Botanique Historique et Palynologie. URA CNRS, Marseille, France. Supplement.
Reimer, P.J., Austin, W.E.N., Bard, E., Bayliss, A., Blackwell, P.G., Bronk Ramsey, C., Butzin, M., Cheng, H., Edwards, R.L., Friedrich, M., Grootes, P.M., Guilderson, T.P., Hajdas, I., Heaton, T.J., Hogg, A.G., Hughen, K.A., Kromer, B., Manning, S.W., Muscheler, R., Palmer, J.G., Pearson, C., van der Plicht, J., Reimer, R.W., Richards, D.A., Scott, E.M., Southon, J.R., Turney, C.S.M., Wacker, L., Adolphi, F., Büntgen, U., Capano, M., Fahrni, S.M., Fogtmann–Schulz, A., Friedrich, R., Köhler, P., Kudsk, S., Miyake, F., Olsen, J., Reinig, F., Sakamoto, M., Sookdeo, A., Talamo, S., 2020. The IntCal20 Northern Hemisphere radiocarbon age calibration curve (0-55 cal kBP). Radiocarbon 62, 725–757. https://doi.org/10.1017/RDC.2020.41.
Safronov, A.N., 2020. Effects of climatic warming and wildfires on recent vegetation changes in the Lake Baikal basin. Climate 8, 57. https://doi.org/10.3390/cli8040057.
Savelieva, L.A., Raschke, E.A., Titova, D.V., 2013. Photographic Atlas of Plants and Pollen of the Lena River Delta. St-Petersburg State University, St-Petersburg (in Russian).
Schulte, L., Meucci, S., Stoof-Leichsenring, K.R., Heitkam, T., Schmidt, N., von Hippel, B., Andreev, A.A., Diekmann, B., Biskaborn, B.K., Wagner, B., Melles, M., Pestryakova, L.A., Alsos, I.G., Clarke, C., Krutovsky, K.V., Herzschuh, U., 2022. *Larix* species range dynamics in Siberia since the Last Glacial captured from sedimentary ancient DNA. Commun. Biol. 5, 570. https://doi.org/10.1038/s42003-022-03455-0.
Shchetnikov, A.A., Klementiev, A.M., Filinov, I.A., Semeney, E.Yu, 2015. Large mammals from the upper Pleistocene reference sections in the Tunka rift valley, Southwestern Baikal region. Stratigr. Geol. Correl. 23, 214–236. https://doi.org/10.1134/S0869593815020057.
Shchetnikov, A.A., Kazansky, A.Y., Filinov, I.A., Matasova, G.G., 2022. Preliminary rock magnetic and paleomagnetic data from a 14.5 m core of Lake Kotokel sediments (Baikal region). In: Kosterov, A., Bobrov, N., Gordeev, E., Kulakov, E., Lyskova, E., Mironova, I. (Eds.), Problems of Geocosmos–2020. Springer Proceedings in Earth and Environmental Sciences. Springer, Cham, pp. 157–177. https://doi.org/10.1007/978-3-030-91467-7_12.
Shichi, K., Takahara, H., Krivonogov, S.K., Bezrukova, E.V., Kashiwaya, K., Takehara, A., Nakamura, T., 2009. Late Pleistocene and Holocene vegetation and climate records from Lake Kotokel, central Baikal region. Quat. Int. 205, 98–110. https://doi.org/10.1016/j.quaint.2009.02.005.
Shichi, K., Takahara, H., Hase, Y., Watanabe, T., Nara, F.W., Nakamura, T., Tani, Y., Kawai, T., 2013. Vegetation response in the southern Lake Baikal region to abrupt climate events over the past 33 cal kyr. Palaeogeogr. Palaeoclimatol. Palaeoecol. 375, 70–82. https://doi.org/10.1016/j.palaeo.2013.02.015.
Shichi, K., Goebel, T., Izuho, M., Kashiwaya, K., 2023. Climate amelioration, abrupt vegetation recovery, and the dispersal of *Homo sapiens* in Baikal Siberia. Sci. Adv. 9, eadi0189. https://www.science.org/doi/10.1126/sciadv.adi0189.
Simonov, E., Kreyndlin, M., Ivanov, A., Panteleeva, I., 2022. Imperiled: The Encyclopedia of Conservation, pp. 389–408. https://doi.org/10.1016/B978-0-12-821139-7.00055-6.
Stockmarr, J., 1971. Tablets with spores used in absolute pollen analysis. Pollen Spores 13, 614–621.
Svensson, A., Andersen, K.K., Bigler, M., Clausen, H.B., Dahl-Jensen, D., Davies, S.M., Johnsen, S.J., Muscheler, R., Parrenin, F., Rasmussen, S.O., Röthlisberger, R., Seierstad, I., Steffensen, J.P., Vinther, B.M., 2008. A 60000 year Greenland stratigraphic ice core chronology. Clim. Past 4, 47–57. https://doi.org/10.5194/cp-4-47-2008.
Talon, B., Payette, S., Filion, L., Delwaide, A., 2005. Reconstruction of the long-term fire history of an old-growth deciduous forest in Southern Québec, Canada, from charred wood in mineral soils. Quat. Res. 64, 36–43. https://doi.org/10.1016/j.yqres.2005.03.003.
Tarasov, P.E., Webb III, T., Andreev, A.A., Afanas'eva, N.B., Berezina, N.A., Bezusko, L. G., Blyakharchuk, T.A., Bolikhovskaya, N.S., Cheddadi, R., Chernavskaya, M.M., Chernova, G.M., Dorofeyuk, N.I., Dirksen, V.G., Elina, G.A., Filimonova, L.V., Glebov, F.Z., Guiot, J., Gunova, V.S., Harrison, S.P., Jolly, D., Khomutova, V.I., Kvavadze, E.V., Osipova, I.M., Panova, N.K., Prentice, I.C., Saarse, L., Sevastyanov, D.V., Volkova, V.S., Zernitskaya, V.P., 1998. Present-day and mid-Holocene biomes reconstructed from pollen and plant macrofossil data from the former Soviet Union and Mongolia. J. Biogeogr. 25, 1029–1053. https://doi.org/10.1046/j.1365-2699.1998.00236.x.
Tarasov, P., Williams, J., Andreev, A., Nakagawa, T., Bezrukova, E., Herzschuh, U., Igarashi, Y., Müller, S., Werner, K., Zheng, Z., 2007. Satellite- and pollen-based quantitative woody cover reconstructions for northern Asia: verification and application to late-Quaternary pollen data. Earth Planet. Sci. Lett. 264, 284–298.
Tarasov, P.E., Andreev, A.A., Anderson, P.M., Lozhkin, A.V., Leipe, C., Haltia, E., Nowaczyk, N.R., Wennrich, V., Brigham-Grette, J., Melles, M., 2013. A pollen-based biome reconstruction over the last 3.562 million years in the Far East Russian Arctic – new insights into climate–vegetation relationships at the regional scale. Clim. Past 9, 2759–2775. https://doi.org/10.5194/cp-9-2759-2013.
Tarasov, P.E., Bezrukova, E.V., Müller, S., Kostrova, S.S., White, D., 2017. Chapter 2: Climate and vegetation history. In: Losey, R.J., Nomokonova, T. (Eds.), Holocene Zooarchaeology of Cis-Baikal, Archaeology in China and East Asia 6. Nünnerich–Asmus Verlag & Media GmbH, Mainz, pp. 15–26.
Tarasov, P.E., Ilyashuk, B.P., Leipe, C., Müller, S., Plessen, B., Hoelzmann, P., Kostrova, S. S., Bezrukova, E.V., Meyer, H., 2019. Insight into the Last Glacial Maximum climate and environments of southern Siberia: a case study from the Baikal region. Boreas 48, 488–506. https://doi.org/10.1111/bor.12330.
Tarasov, P.E., Leipe, C., Wagner, M., 2021. Environments during the spread of anatomically modern humans across Northern Asia 50-10 cal. kyr BP: What do we know and what would we like to know? Quat. Int. 596, 155–170. https://doi.org/10.1016/j.quaint.2020.10.030.
Tinner, W., Conedera, M., Ammann, B., Gäaggeler, H.W., Gedye, S., Jones, R., Sägesser, B., 1998. Pollen and charcoal in lake sediments compared with historically documented forest fires in southern Switzerland since AD 1920. Holocene 8, 31–42. https://doi.org/10.1191/095968398667205430.
Tinner, W., Conedera, M., Ammann, B., Lotter, A.F., 2005. Fire ecology north and south of the Alps since the last ice age. Holocene 15, 1214–1226. https://journals.sagepub.com/doi/10.1191/0959683605hl892rp.
Umbanhowar Jr., C.E., 1996. Recent fire history of the northern Great Plains. Amer. Midl. Nat. 135, 115–121.
Vasil'ev, S.A., Kuzmin, Y.V., Orlova, L.A., Dementiev, V.N., 2002. Radiocarbon-based chronology of the Paleolithic of Siberia and its relevance to the peopling of the New World. Radiocarbon 44, 503–530. https://doi.org/10.1017/S0033822200031878.
Walker, M., Head, M.J., Berkelhammer, M., Björck, S., Cheng, H., Cwynar, L., Fisher, D., Gkinis, V., Long, A., Lowe, J., Newnham, R., Rasmussen, S.O., Weiss, H., 2018. Formal ratification of the subdivision of the Holocene series/epoch (Quaternary system/period): two new global boundary stratotype sections and points (GSSPs) and three new stages/subseries. Episodes J. Int. Geosci. 41, 213–223. https://doi.org/10.18814/epiiugs/2018/018016.
Wang, Y., Goring, S.J., McGuire, J.L., 2019. Bayesian ages for pollen records since the last glaciation in North America. Sci. Data 6, 176. https://doi.org/10.1038/s41597-019-0182-7.
Wang, Y., Pedersen, M., Alsos, I., de Sanctis, B., Racimo, F., Prohaska, A., Coissac, É., Owens, H., Merkel, M., Fernandez-Guerra, A., Rouillard, A., Lammers, Y., Alberti, A., Denoeud, F., Money, D., Ruter, A., McColl, H., Larsen, N., Cherezova, A., Edwards, M.E., Fedorov, G.B., Haile, J., Orlando, L., Vinner, L., Korneliussen, T.S., Beilman, D.W., Bjørk, A.A., Cao, J., Dockter, C., Esdale, J., Gusarova, G., Kjeldsen, K. K., Mangerud, J., Rasic, J.T., Skadhauge, B., Svendsen, J.I., Tikhonov, A., Wincker, P., Xing, Y., Zhang, Y., Froese, D.G., Rahbek, C., Bravo, D.N., Holden, P.B., Edwards, N.R., Durbin, R., Meltzer, D.J., Kjær, K.H., Möller, P., Willerslev, E., 2021. Late Quaternary dynamics of Arctic biota from ancient environmental genomics. Nature 600, 86–92. https://doi.org/10.1038/s41586-021-04016-x.
Wang, Z., Huang, J.-G., Ryzhkova, N., Li, J., Kryshen, A., Voronin, V., Li, R., Bergeron, Y., Drobyshev, I., 2021. 352 years long fire history of a Siberian boreal forest and its primary driving factor. Global Planet. Change 207, 103653. https://doi.org/10.1016/j.gloplacha.2021.103653.
Wang, Z., Fang, K., Yao, Q., 2022. Fire history and its forcing in Northeastern Asia boreal forests. Nat. Hazards Res. 2, 166–171. https://doi.org/10.1016/j.nhres.2022.07.001.
Weber, A.W., 2020. Middle Holocene hunter–gatherers of Cis-Baikal, Eastern Siberia: combined impacts of the boreal forest, bow-and-arrow, and fishing. Archaeol. Res. Asia 24, 100222. https://doi.org/10.1016/j.ara.2020.100222.
Whitlock, C., Larsen, C., 2001. Charcoal as a fire proxy. In: Smol, J.P., Birks, H.J.B., Last, W.M., Bradley, R.S., Alverson, K. (Eds.), Tracking Environmental Change Using Lake Sediments 3: Terrestrial, Algal, and Siliceous Indicators. Springer, Dordrecht, pp. 75–97. https://doi.org/10.1007/0-306-47668-1_5.
Yasunari, T.J., Narita, D., Takemura, T., Wakabayashi, S., Takeshima, A., 2024. Comprehensive impact of changing Siberian wildfire severities on air quality, climate, and economy: MIROC5 global climate model's sensitivity assessments. Earth's Future 12, e2023EF004129. https://doi.org/10.1029/2023EF004129.
Zhang, Y., Wünnemann, B., Bezrukova, E.V., Ivanov, E.V., Shchetnikov, A.A., Nourgaliev, D., Levina, O., 2013. Basin morphology and seismic stratigraphy of Lake Kotokel, Baikal region, Russia. Quat. Int. 290–291, 57–67. https://doi.org/10.1016/j.quaint.2012.11.029.
Zouhar, K., 2021. Fire regimes of plains grassland and prairie ecosystems. In: Fire Effects Information System. U.S. Department of Agriculture, Forest Service, Rocky Mountain Research Station, Missoula Fire Sciences Laboratory (Producer) [Online]. www.fs.usda.gov/database/feis/fire_regimes/PlainsGrass_Prairie/all.html. (Accessed 14 April 2024).